

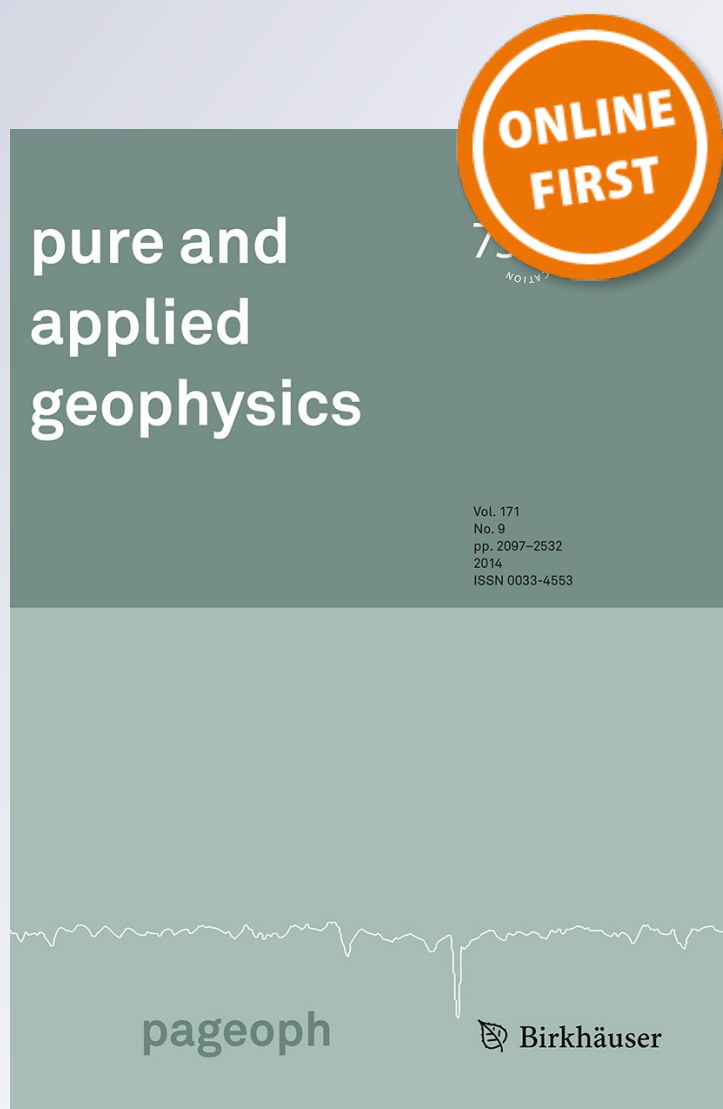
Fault Geometry and Active Stress from Earthquakes and Field Geology Data Analysis: The Colfiorito 1997 and L'Aquila 2009 Cases (Central Italy)

F. Ferrarini, G. Lavecchia, R. de Nardis & F. Brozzetti

Pure and Applied Geophysics
pageoph

ISSN 0033-4553

Pure Appl. Geophys.
DOI 10.1007/s00024-014-0931-7



Your article is protected by copyright and all rights are held exclusively by Springer Basel. This e-offprint is for personal use only and shall not be self-archived in electronic repositories. If you wish to self-archive your article, please use the accepted manuscript version for posting on your own website. You may further deposit the accepted manuscript version in any repository, provided it is only made publicly available 12 months after official publication or later and provided acknowledgement is given to the original source of publication and a link is inserted to the published article on Springer's website. The link must be accompanied by the following text: "The final publication is available at link.springer.com".

Fault Geometry and Active Stress from Earthquakes and Field Geology Data Analysis: The Colfiorito 1997 and L'Aquila 2009 Cases (Central Italy)

F. FERRARINI,¹ G. LAVECCHIA,¹ R. DE NARDIS,^{1,3} and F. BROZZETTI²

Abstract—The fault segmentation pattern and the regional stress tensor acting since the Early Quaternary in the intra-Appennine area of central Italy was constrained by integrating two large geological and seismological fault-slip data sets collected for the areas struck by the two most energetic seismic sequences of the last 15 years (Colfiorito 1997, M_w 6.0 and L'Aquila 2009, M_w 6.1). The integrated analysis of the earthquake fault association and the reconstruction of the 3D shape of the seismogenic sources were exploited to identify homogeneous seismogenic volumes associated with subsets of geological and focal mechanism data. The independent analysis of geological and seismological data allowed us to observe and highlight similarities between the attitude of the long-term (e.g., Quaternary) and the instantaneous present-day (seismogenic) extensional deformations and to reveal their substantial coaxiality. Coherently, with the results from the kinematic analysis, the stress field inversion also noted a prevailing tensional seismotectonic regime associated with a sub-horizontal, NE–SW, minimum stress axis. A minor, very local, and shallow (<5 km) strike-slip component of the stress field was observed in the Colfiorito sector, where an inherited N–S oriented right-lateral fault was reactivated with sinistral kinematics. Instead, an almost total absence of strike-slip solutions was observed in the L'Aquila area. These results do not agree with those indicating Quaternary regional strike-slip regimes or wide areas characterized by strike-slip deformation during the Colfiorito and L'Aquila seismic sequences.

Key words: L'Aquila and Colfiorito earthquakes, structural analysis, kinematic analysis, stress inversion, active deformation, central Italy.

1. Introduction

The inversion of fault-slip data and focal mechanisms is commonly used to infer the orientation and relative magnitude of the principal stress or

deformation axes in tectonically active areas (TWISS and UNRUH 1998). Previous investigations in central Italy dealt with this subject at different scales, focusing on the active strain and stress fields from seismological and geodetic data, from borehole breakouts and numerical modelling (D'AGOSTINO *et al.* 2009; DEVOTI *et al.* 2011; MONTONE *et al.* 2012; PIERDOMINICI and HEIDBACH 2012; CARAFA and BARBA 2013, FERRARINI *et al.* 2013). Starting with the Norcia 1979 earthquake (M_w 5.8), the following Gubbio 1984 (M_w 5.6) and Barrea 1984 (M_w 5.9) extensional events, structural-kinematic data concerning the outcropping Quaternary fault system were acquired and inverted to constrain the long-term stress field and to compare it with the seismological one (BROZZETTI and LAVECCHIA 1994; BONCIO *et al.* 1996; CELLO *et al.* 1997; BONCIO and LAVECCHIA 2000a, b; PACE *et al.* 2002). Due to the poor quality of the seismological data available at the time of these events, the process of linking faults and earthquakes was not straightforward. The noticeable quality improvement of the hypocentral locations (CHIARALUCE *et al.* 2003, 2011a, b) concerning two energetic seismic sequences that occurred in central Italy in the last 20 years (Colfiorito 1997, M_w 6.0 and L'Aquila 2009, M_w 6.1), together with detailed structural analyses carried out in the epicentral areas (CALAMITA *et al.* 1999; BARBA and BASILI 2000; BONCIO and LAVECCHIA 2000a; CHIARALUCE *et al.* 2005; BARCHI and MIRABELLA 2009; LAVECCHIA *et al.* 2012), improved the understanding of the geometric relationships between the geological and the seismological sources. In addition, the kinematics of the seismogenic faults was constrained by large data sets of focal mechanisms (CHIARALUCE *et al.* 2004; HERRMANN *et al.* 2011).

¹ Laboratorio di Geodinamica e Sismogenesi, DiS.P.U.Ter, Università "G. d'Annunzio", Campus Universitario, Chieti Scalo, 66013 Chieti, Italy. E-mail: f.ferrarini@unich.it

² Laboratorio di Geologia Strutturale e Cartografia Geologica, DiS.P.U.Ter, Università "G. d'Annunzio", Campus Universitario, Chieti Scalo, 66013 Chieti, Italy.

³ Dipartimento della Protezione Civile, Rome, Italy.

The active stress tensor derived from the inversions of geological and/or seismological fault-slip data showed a dominant SW–NE oriented tensional stress field in both the Colfiorito and L'Aquila areas, which is consistent with the regional tectonic regime that has been active in central Italy since the Quaternary (BONCIO *et al.* 2000; HUNSTAD *et al.* 2003; BARBA *et al.* 2008; D'AGOSTINO *et al.* 2009; DEVOTI *et al.* 2011; LAVECCHIA *et al.* 2012; MONTONE *et al.* 2012; PIERDOMINICI and HEIDBACH 2012). Nevertheless, some authors have stressed an important role that should be played by the strike-slip tectonics at local and regional scales during the Quaternary. CELLO *et al.* (1997) hypothesised the existence of deep-seated, N–S striking, left-lateral shear zones that would have controlled the extensional processes in the Umbria-Marche area. CARAFA and BARBA (2011) attributed the transcurrent deformation along the Apennine belt to changes in the strength of the lithosphere, which would control the onset of strike-slip/reverse-strike earthquakes along the lateral ramps of the main thrusts. ELTER *et al.* (2012) interpreted the central Italy intra-mountain basins as extensional pull apart structures and described their NW–SE trending boundary faults as strike-slip faults. These features would represent synthetic riedels of a main NNW–SSE oriented deep-seated sinistral shear zone. Still, based on the inversion of a large data set of focal mechanisms, D'AMICO *et al.* (2013) noted a prevailing strike-slip stress field in a large portion of the L'Aquila 2009–2012 seismic sequence (Campotosto-Mt. Gorzano and Montereale sectors).

In this paper, we aim to constrain the regional stress tensor acting since the Early Quaternary in the L'Aquila and Colfiorito areas by using a large amount of original geological data and exploring the possibility of local stress tensor deviations due to preexisting discontinuities. In fact, the research is carried out through the close integration of geological and seismological data. The earthquake data (mainly hypocentral locations and fault plane solutions) are derived from the literature, whereas the geological fault-slip data are mostly new. The 3D geometry and the segmentation pattern of the fault system involved in the L'Aquila 2009 seismic sequence are from LAVECCHIA *et al.* (2012), whereas those of the Colfiorito 1997 seismic sequence are reconstructed here

following the same approach. For both the L'Aquila and Colfiorito areas, we perform a kinematic analysis and a formal stress inversion of the two independent geological and seismological data sets related to a large portion of the active central Apennine belt. The similarities and/or inconsistencies between the long-term geological and the present-day instantaneous seismological stress tensors have been investigated and analysed.

2. Seismotectonic Setting

The Apennine mountain belt of central Italy is crosscut by a NW–SE striking extensional system of normal and normal-oblique faults active since the Early Quaternary (Fig. 1) (LAVECCHIA 1988; CALAMITA *et al.* 1994; VALENSISE and PANTOSTI 2001; LAVECCHIA *et al.* 2002). The extensional fault system, along which most of the seismicity is concentrated (Fig. 1, see also the lower left inset), offsets the preexisting compressive and strike-slip structures of the Umbria-Marche-Abruzzi Mio-Pliocene fold-and-thrust belt (LAVECCHIA *et al.* 1994) and locally generates intra-mountain depressions (GALADINI and GALLI 2000; BONCIO and LAVECCHIA 2000a; ROMANO *et al.* 2013).

The extensional faults, which mainly dip southwestward, are arranged along major extensional alignments hereinafter identified as the internal, intermediate, and external alignments (blue, red, and green double lines in Fig. 1 from LAVECCHIA *et al.* 2011a, b). The fault alignments may reach lengths of hundreds of kilometres (see, e.g., composite sources in DISS WORKING GROUP 2010), and the individual en echelon fault segments typically extend 20–25 km along a strike and 10–15 km along a dip (BONCIO *et al.* 2004).

The epicentral area of the Colfiorito sequence occurs along a fault alignment developing from Gubbio to Colfiorito and, further south, from Norcia to L'Aquila (intermediate west-dipping Quaternary fault alignment in Figs. 1, 2). Thus, the epicentral area of the L'Aquila sequence occurs along this same alignment and the Mt. Gorzano fault (G). The latter belongs to the more external alignment, which extends from the Mt. Vettore (V) to the Gran Sasso

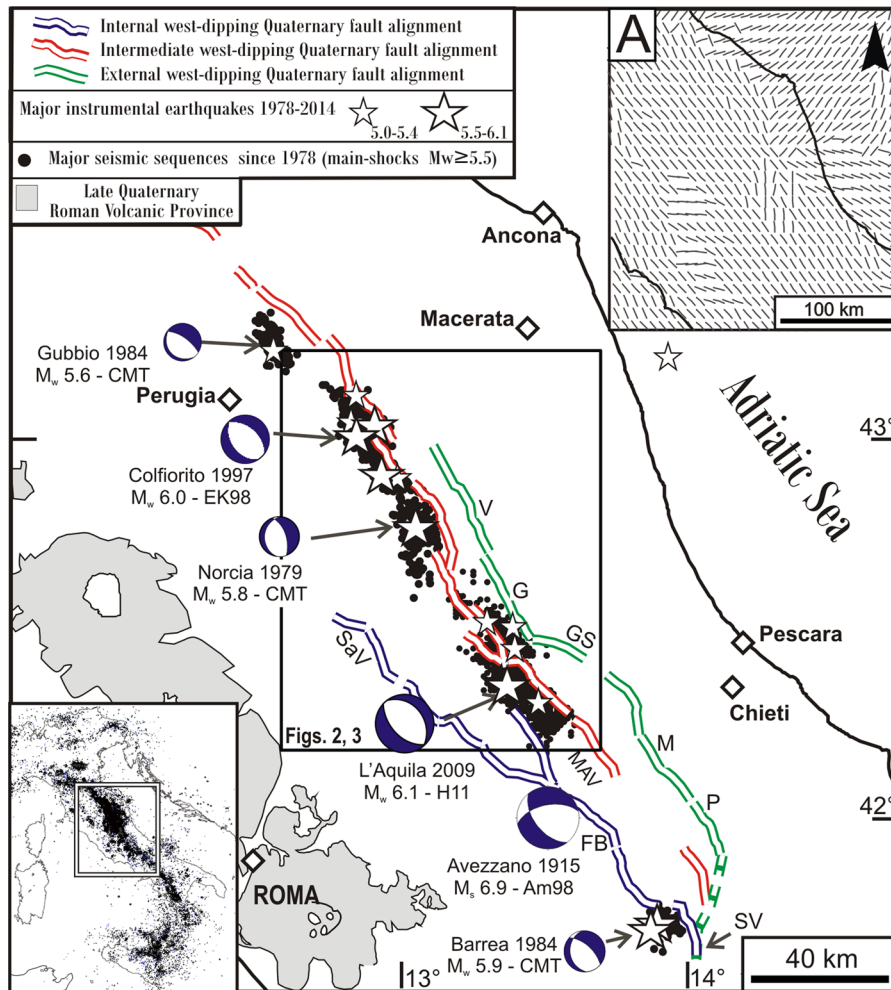


Figure 1

Extensional seismogenic fault alignments and major instrumental sequences in central Italy (mainshocks $M_w \geq 5.5$): Gubbio, 1984; Colfiorito, 1997; Norcia, 1979; L'Aquila, 2009; Barrea, 1984. The Avezzano focal mechanism (AM98) is from AMORUSO *et al.* (1998); the Colfiorito solution (EK98) is from EKSTRÖM *et al.* (1998); the L'Aquila, Mt. Gorzano and Ocre solutions (H11) are from HERRMANN *et al.* (2011); the other solutions (CMT) are from the HARVARD CMT database (available at <http://www.globalcmt.org>). Acronyms along the internal fault alignment (blue lines): SaV Salto Valley, FB Fucino Basin, SV Sangro Valley; along the intermediate alignment (red lines): MAV Middle Aterno Valley; along the external alignment (green lines): V Mt. Vettore, G Mt. Gorzano, GS Gran Sasso ridge, M Mt. Morrone, P Mt. Porrara. The Sh_{max} directions (upper right inset) are from CARAFA and BARBA (2013). The location map (lower left inset) represents the instrumental seismicity recorded from 2005 to 2013, as reported in the ISIDE database (<http://iside.rm.ingv.it/iside/standard/index.jsp>)

ridge (GS) and, further south, to the Mt. Morrone-Mt. Porrara area (M and P) (Figs. 1, 2B). A third extensional fault alignment, not involved in the seismic activity of the Colfiorito and L'Aquila sequences, extends in a more internal position from the Salto Valley (SaV) to the Fucino Basin (FB) and the Sangro Valley (SV) (Fig. 1). During the last 100 years, two major ($M_w \geq 5.5$) events struck the internal alignment (Avezzano 1915, M_s 6.9; Barrea 1984, M_w 5.9). Many moderate earthquakes were instead

associated with the intermediate alignment (Gubbio 1984, M_w 5.6; Colfiorito 1997, M_w 6.0; Norcia 1979, M_w 5.9; L'Aquila 2009, M_w 6.1) (LAVECCHIA *et al.* 2011a, b and reference therein). The focal mechanisms (Figs. 1, 2A) consistent within a regional NE–SW tensional stress field that has been active in the region at least since the Early Quaternary (BONCIO *et al.* 2000). The present-day strain field detected from GPS data and borehole breakouts is characterized by

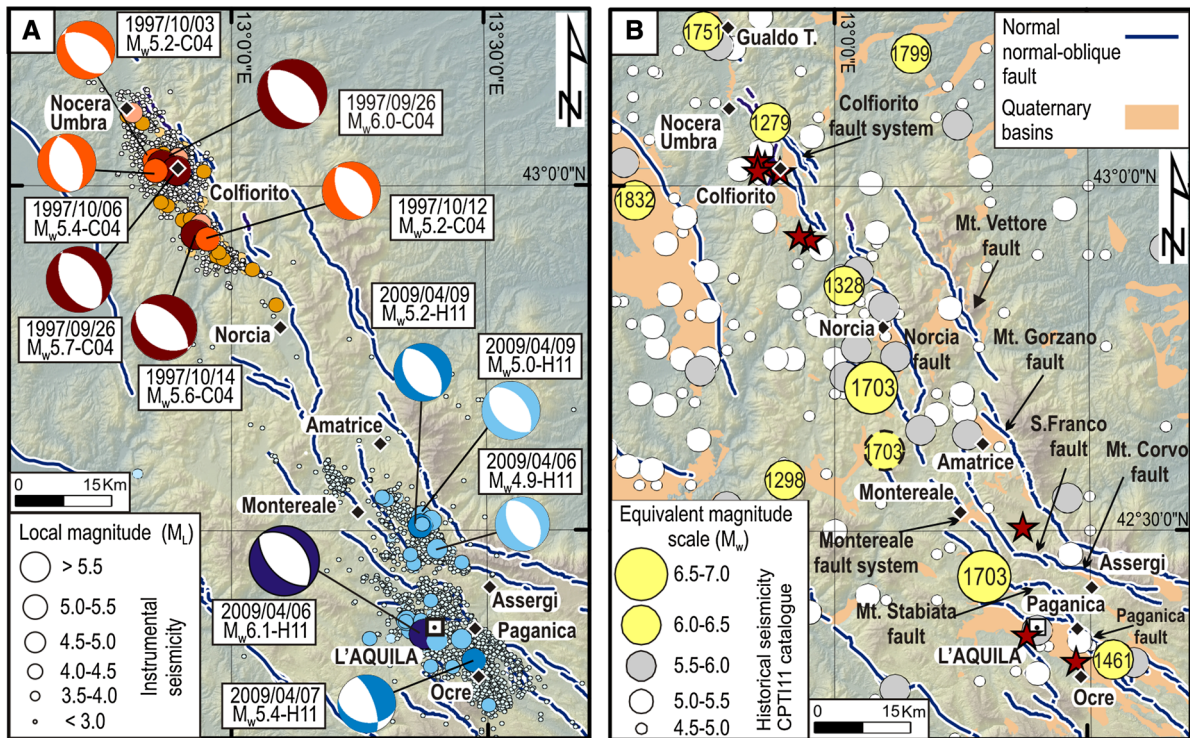


Figure 2

Epicentre distribution of historical and instrumental earthquakes within the study areas. **A** Instrumental earthquakes with $M_L \geq 2.4$ that occurred during the Colfiorito 1997 (red scale symbols) and L'Aquila 2009 seismic sequences (blue scale symbols) as extracted from CHIARALUCE *et al.* (2003) and CHIARALUCE *et al.* (2011a), respectively. Focal mechanisms refer to major earthquakes ($M_w \sim \geq 5.0$) that occurred during the two sequences: C04—from CHIARALUCE *et al.* (2004); H11—from HERMANN *et al.* (2011). **B** Historical earthquakes in the time interval 1000–1996 A.D. (in the central Apennines) extracted from the CPTI11 parametric catalogue (ROVIDA *et al.* 2011); the year of occurrence for the major historical events is reported. Red stars represent the main instrumental earthquakes ($M_w \sim \geq 5.0$) of the Colfiorito 1997 and L'Aquila 2009 seismic sequences as reported in **A**. The fault symbols and names are the same for both figures

a similar extensional pattern. The velocity field estimated from GPS data is approximately 2 mm/a in the Umbria-Marche Apennines and increases to 3 mm/a in the Abruzzo Apennines (HUNSTAD *et al.* 2003; D'AGOSTINO *et al.* 2009; GALVANI *et al.* 2012).

The historical earthquakes (GUIDOBONI *et al.* 2007; ROVIDA *et al.* 2011) in the area involved with the Colfiorito 1997 and L'Aquila 2009 sequences are reported in the map of Fig. 2B. In the last 1,000 years, before the 1997 Colfiorito earthquake, seven events with $M_w \geq 6.0$ are known to have occurred mainly along the intermediate extensional alignment (Fig. 1). From north to south, they are dated as follows: July 27, 1751 (M_w 6.2), April 30, 1279 (M_w 6.3), December 1, 1328 (M_w 6.4), January 14, 1703 (M_w 6.7), January 16, 1703 (M_w 6.0), February 2, 1703 (M_w 6.7), and November 27, 1461 (M_w 6.4). The 1751, 1279 and 1328 events

may be attributed to the Colfiorito fault system. The three 1703 events are described by GALLI *et al.* (2010) as a SE-propagating multiple-rupture seismic sequence which activated, from north to south, the WSW-dipping Norcia, Montereale and Pizzoli faults (LAVECCHIA *et al.* 2012 and references therein). In addition, it possibly involved the Paganica fault, e.g., the master fault of the 2009 L'Aquila earthquake (M_w 6.3) (BONCIO *et al.* 2010), which was also responsible for the 1461 event (CINTI *et al.* 2011).

3. Structural-Kinematic Analysis of the Colfiorito and L'Aquila Fault Systems

To investigate the active fault geometry and kinematics in the Colfiorito and L'Aquila epicentral

areas, we collected and analysed a large number of fault-slip data along all the major outcropping Quaternary faults. Most of the data are original with the exception of some outcrops in the Colfiorito and Norcia areas (BROZZETTI and LAVECCHIA 1994; BONCIO *et al.* 2000; LAVECCHIA *et al.* 2012). The surveyed sites are reported in the maps of Fig. 3; the geological parameters and the fault planes and associated

slickenlines are summarised in the Table 1 and in the stereoplots of Fig. 4A, B (lower hemisphere Schmidt nets), respectively.

3.1. The Colfiorito Fault System

The SW-dipping Colfiorito normal fault system is arranged in three major en echelon fault segments

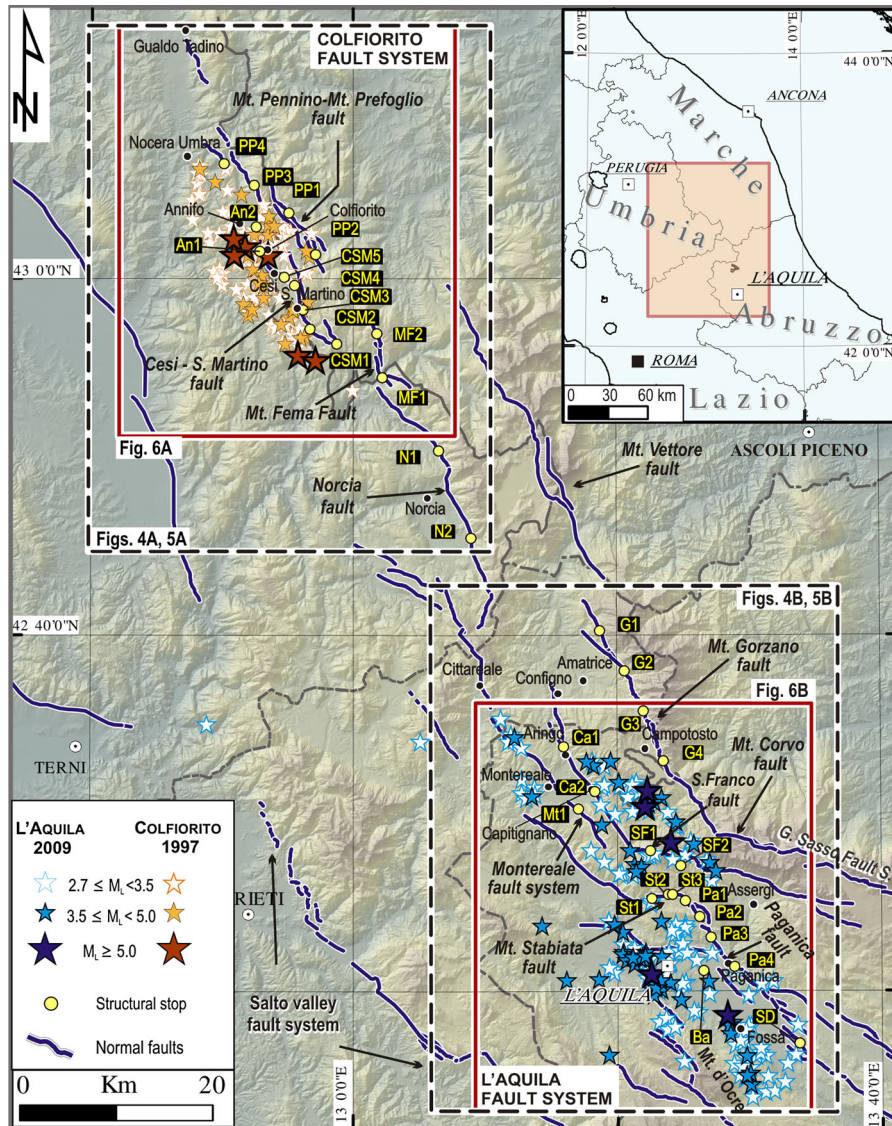


Figure 3

Location map of the geological and seismological data analysed in this paper. Yellow dots represent the location of structural data plotted in Fig. 4; the star symbols represents the epicentral distribution of the $M_L \geq 2.7$ focal mechanisms of the Colfiorito 1997 and L'Aquila 2009 seismic sequences (CHIARALUCE *et al.* 2004; HERMANN *et al.* 2011, respectively) used for the kinematics analysis in Fig. 6. Black bolded stars highlight the events selected for the stress inversion ($M_L \geq 3.5$)

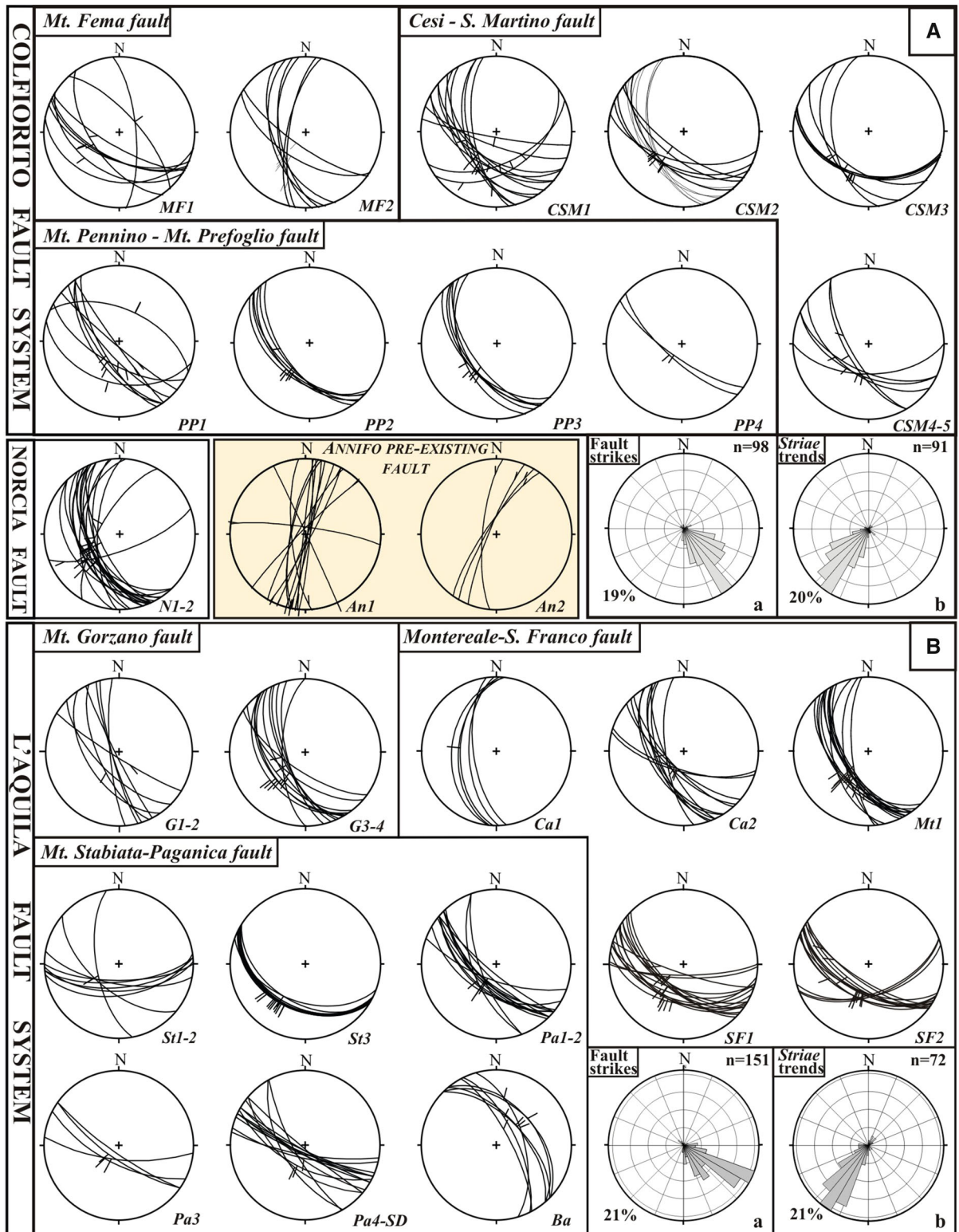


Figure 4

Fault-slip data collected in the investigated areas belonging to the Colfiorito and L'Aquila fault systems. The Schmidt nets' lower projections of the fault planes and slickenlines are plotted. The rose diagrams **a**, **b** summarize the fault and striae trends of the analysed fault systems. The acronyms of the structural stops, as reported in Fig. 3, are on the bottom-right of each plot

aligned in an average NW–SE direction: the Mt. Pennino-Mt. Prefoglio, Cesi-S. Martino and Mt. Fema faults (Figs. 3, 4A).

The Mt. Pennino-Mt. Prefoglio segment, which is the longest one, extends for approximately 18 km along the NW–SE direction and dips 45° – 85° south-westward. In turn, it consists of two subparallel right-stepping en echelon faults characterised by prevailing normal kinematics with a subordinate left lateral component (stops PP1, PP2, PP3, and PP4 in Figs. 3, 4A).

The Cesi-S. Martino segment strikes for approximately 12 km along a mainly NW–SE direction and dips south-westward with a 45° – 85° dip angle. Locally, the fault plane shows subordinate bending in a near E–W direction (stops CSM1, CSM2, CSM3, CSM4, and CSM5 in Figs. 3, 4A).

The Mt. Fema segment consists of three small minor normal faults with a total length of approximately 8 km striking along a $N130^{\circ}$ direction and dipping 40° – 80° to the southwest. Kinematic data show a main direction of extension oriented NE–SW (stops MF1 and MF2 in Figs. 3, 4A), even if subordinate slip vectors oriented nearly NNE–SSW also occur (see MF2 in Fig. 4A).

Along the northward continuation of the Cesi-San Martino segment, a northward 10° E-striking strike-slip fault segment, hereinafter referred to as the Annifo fault, outcrops. The Annifo fault-slip data (stops An1 and An2 in Figs. 3, 4A) do not show a normal fault deformation but rather N–S right-lateral kinematics, which possibly developed during the compressional phase affecting the Umbria-Marche Apennines in the Late Miocene (LAVECCHIA *et al.* 1988; DEIANA and PIALLI 1994). We focused on such a structural element because it geographically coincides with the N–S trending microseismicity that excited the Annifo basin during the Colfiorito seismic sequence (Mt. Pennino-Ricciano fault in CHIARALUCE *et al.* 2005). Our field survey did not highlight any surface evidence of fault reactivation with left-lateral kinematics (compatible with the active extensional regime) even if, east of the S. Martino village, some evidence of reactivation with normal-oblique kinematics was described by CELLO *et al.* (1997).

New fault slip data were also collected along the Norcia normal fault, which outcrops in an

intermediate position between the Colfiorito and L'Aquila fault systems (stops N1 and N2 in Figs. 3, 4). The Norcia fault, which is slightly shifted westwards with respect to the Mt. Fema fault, extends for nearly 30 km along strike and exhibits a general $N160^{\circ}$ -trending 45° – 70° dip and prevailing normal kinematics.

As a whole, the Colfiorito and Norcia fault-slip data set consists of 98 fault planes trending from WNW–ESE to NNW–SSE with the maximum data frequency (19 %) falling between $N140^{\circ}$ and $N150^{\circ}$ (rose diagram in Fig. 4Aa). Moreover, the striation trend ($n = 91$) shows a maximum distribution around a $N220^{\circ}$ – $N240^{\circ}$ direction ($\sim 40\%$ data) that is perfectly consistent with the NE–SW regional extension direction (rose diagram in Fig. 4Ab).

3.2. The L'Aquila Fault System

The SW-dipping normal faults belonging to the L'Aquila system are aligned in an average $N130^{\circ}$ direction (Figs. 3, 4B), with subordinate E–W and NNW–SSE trending segments that dip south and west, respectively. Here, we will focus on the structural data belonging to the main fault segments activated during the L'Aquila 2009 sequence, which are the Mt. Gorzano, the Montereale, and the Paganica-Mt. Stabiata faults (Figs. 3, 4B) (LAVECCHIA *et al.* 2012).

The Mt. Gorzano fault extends continuously for ~ 28 km, striking $N140^{\circ}$ – 150° and dipping 60° – 70° to the WSW (stops G1, G2, G3, and G4 in Figs. 3, 4B). In the surroundings of Campotosto, the fault attitude slightly changes, striking $N155^{\circ}$ – 165° and dipping steeply (80° – 85°) to the WSW. To the south, the fault intersects the E–W-striking, S-dipping Mt. Corvo segment of the Gran Sasso normal fault system. The fault kinematics is mostly dip-slip with a minor left-lateral component, and the slip vectors mainly plunge toward $N220^{\circ}$ – 230° .

The Montereale fault system is arranged in a number of minor segments. The easternmost one outcrops from the Configno village to the Mt. S. Franco fault (~ 25 km); the westernmost, in the surroundings of the Montereale and Capitignano villages. The fault plane strikes mainly $N120^{\circ}$ – 150° (stops Ca1, Ca2, Mt1, SF1, and SF2 in Figs. 3, 4B) with dip-angles ranging from 50° to 70° . Some exceptions

occur in the sector of the Mt. S. Franco fault, where some E–W trending planes were surveyed. Measured slickenlines confirm prevailing dip-slip kinematics with minor left-lateral or right-lateral components on planes roughly N–S or E–W oriented, respectively.

The Paganica-Mt. Stabiata fault consists of two different trending segments: the NW–SE oriented segment, which represents the longer one (~ 18 km) and dips south-westwards, and the E–W trending one, which strikes for approximately 6 km in the Mt. Stabiata area and dips southwards. Most of the fault planes show a $N120^\circ$ – 130° direction and a 55° – 75° dip angle (stops St1, St2, St3, Pa1, Pa2, Pa3, Pa4, and SD in Figs. 3, 4B). Slickenlines highlight dip-slip kinematics consistent with NE–SW oriented extension. Some minor antithetic planes, such as the Bazzano one (stop Ba in Figs. 3, 4B), are also observable in the hanging-wall block of the Paganica-Mt. Stabiata fault showing compatible kinematics with the latter.

The overall L'Aquila system's fault planes ($n = 151$) range in strike from WNW–ESE to NNW–SSE, with the maximum data frequency ($\sim 40\%$ data) falling between $N110^\circ$ and $N130^\circ$ (rose diagram in Fig. 4Ba). In addition, the striation trend ($n = 72$) shows a maximum distribution around a $N200^\circ$ – $N225^\circ$ direction (more than 50% data in the rose diagram in Fig. 4Bb), which is consistent with prevailing pure dip-slip kinematics.

The fault planes show strike variations both locally and along major segments, as is the case for the Mt. S. Franco and Mt. Stabiata E–W trending faults (stops SF1, SF2, St1, and St2 in Figs. 3, 4B) and the Montereale fault (stops Ca1 and Mt1 in Figs. 3, 4B). Nevertheless, the respective slickenlines often reveal kinematics consistent with a general extension oriented in a SW–NE direction. This feature possibly suggests that these structures were inherited by earlier tectonic phases (PIZZI and GALADINI 2009).

4. The Colfiorito 1997 and L'Aquila 2006 Seismic Sequences

4.1. The Colfiorito 1997 Sequence

The Colfiorito 1997 sequence spreads for almost 50 km along a NW–SE direction from Nocera Umbra

to 5 km north of Norcia. From September 26 to November 3, 1997, the sequence was characterized by more than 1500 earthquakes and six events with $5.2 \leq M_w \leq 6.0$ that nucleated in the 1–10 km depth range. The seismicity involved different segments pertaining to the SW-dipping Colfiorito active fault system (Figs. 2A, 5A, epicentres from CHIARALUCE *et al.* 2003). The sequence began with a M_w 4.5 foreshock on September 3, 1997 (CHIARALUCE *et al.* 2004 and references therein) and was followed by two mainshocks of M_w 5.7 and M_w 6.0 on September 26, both nucleating on the SW-dipping Mt. Pennino-Mt. Prefoglio fault at a distance of nearly 3 km from each other. After these two energetic events, some evidence of surface breaks was observed and controversially interpreted as secondary induced effects or as a direct expression of fault rupture (CELLO *et al.* 1997, 2000; BASILI *et al.* 1998; CINTI *et al.* 1999; GALLI and GALADINI 1999; MEGHRAOUI *et al.* 1999; VITTORI *et al.* 2000). In early October, the seismicity started to activate the SW-dipping Cesi-S. Martino fault segment (CHIARALUCE *et al.* 2003), where two shocks nucleated on October 3 (M_w 5.2) and 6 (M_w 5.4). Two other large shocks nucleated further southeast on October 12 and 14, 1997 (M_w 5.2 and M_w 5.6, respectively), at the southern tip of the same fault, and/or activating a third independent segment (BARBA and BASILI 2000). The focal mechanisms show normal and normal-oblique kinematics (Fig. 2b) consistent with a nearly horizontal tensional axis oriented SW–NE (EKSTRÖM *et al.* 1998; CHIARALUCE *et al.* 2004). Conversely, on October 16, an M_w 4.3 earthquake with almost pure strike-slip kinematics and showing a WSW–ENE oriented T-axis nucleated close to the Annifo N–S fault zone (upper right inset in Fig. 5A).

During 1998, the seismic activity moved north-westward, activating the SW-dipping Gualdo Tadino fault with an M_w 5.1 event at a depth of 6–7 km on April 3 (PONDRELLI *et al.* 2002; CIACCIO *et al.* 2005). This normal-faulting earthquake represents the last important event of the 6-month long Colfiorito seismic crisis.

4.2. The L'Aquila 2009 Sequence

In the time interval from March 30 to December 29, the L'Aquila 2009 sequence (Fig. 2A), similarly to the

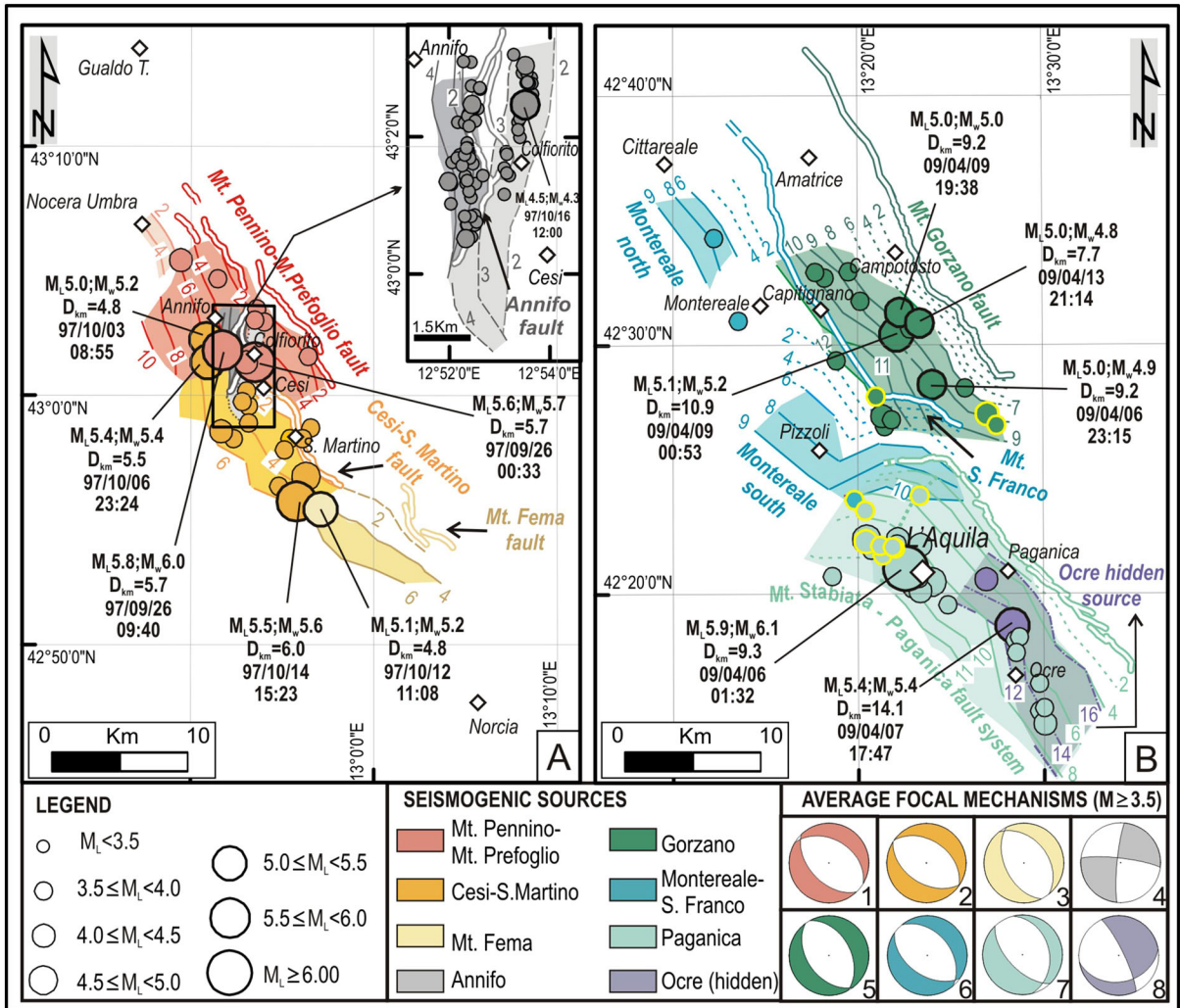


Figure 5

Depth-contour lines of the seismogenic fault planes involved in the A-Colfiorito 1997 (orange-yellow shades) and B-L'Aquila 2009 (blue-green shades) seismic sequences as reconstructed on the basis of the aftershock distribution (see text for details); the depth-contour lines of the Annifo small seismogenic source are also drawn (grey shades in the upper right inset). The continuous depth-contour lines refer to the observed seismogenic patches (coloured areas); the dashed-lines represent the inferred fault-links between the seismogenic patches and the outcropping faults. The identified individual fault segments are differently coloured and numbered from 1 to 8 (1 Mt. Pennino-Mt. Prefoglio, 2 Cesi-S. Martino, 3 Mt. Fema, 4 Annifo, 5 Mt. Gorzano, 6 Montereale-Mt. S. Franco, 7 Paganica-Mt. Stabiata, 8 hidden Ocre). The epicentres of the events ($M_L \geq 3.5$) used to compute the average focal mechanism (Bingham statistics) representative of each distinguished fault source are reported in map view. The yellow bold epicentres highlight the activation of fault portions characterized by structural complexities (see Sect. 7.3 for detail)

Colfiorito 1997 one, spread for nearly 50 km along an average NW–SE direction from the Cittareale village to approximately 10 km SE of the Paganica village (CHIARALUCE *et al.* 2011a). The sequence was characterized by five shocks with $M_w \sim \geq 5.0$ (Figs. 2A, 5B) and more than 2,600 earthquakes that nucleated mainly in the first 15 km depth interval.

The April 6 mainshock (M_w 6.1) and its largest foreshock (March 30, M_w 4.0) activated the SW-dipping Paganica-Mt. Stabiata normal fault (LAVECCHIA *et al.* 2012). The earthquake nucleated at a depth of ~ 9 km and was characterized by unilateral south-eastward propagating rupture (CIRELLA *et al.* 2009; PINO and DI LUCCIO 2009) associated with coseismic

ground deformation (ANZIDEI *et al.* 2009; BONCIO *et al.* 2010; EMERGEO WORKING GROUP 2009; FALCUCCI *et al.* 2009). A second mainshock (April 7, M_w 5.4) nucleated in the Ocre Mts. area at a depth of ~ 14 km, while a third one (April 9, M_w 5.2) nucleated on the SW-dipping Mt. Gorzano fault, striking the Campotosto-Amatrice sector (Fig. 5B). The focal mechanisms showed normal and normal-oblique kinematics (Fig. 2A) consistent with a nearly horizontal tensional axis oriented SW–NE to WSW–ENE (HERRMANN *et al.* 2011).

From 2009 to 2012, recurrent low-magnitude seismic activity (M_w up to 3.6) occurred on the overall 2009 epicentral area and migrated northwest towards the Cittareale and Montereale villages (ISIDE, <http://iside.rm.ingv.it/iside/standard/index.jsp>). This seismicity can be related to the activation of the Montereale -S. Franco fault, located between the Paganica and the Mt. Gorzano faults at depths between 5 and 15 km (LAVECCHIA *et al.* 2012).

5. Geometry of the Colfiorito 1997 and L'Aquila 2009 Seismogenic Sources

The close geometric integration of the surface fault segmentation pattern with the high-quality location of the seismicity is a useful tool to infer the 3D geometry of the seismogenic sources. Such an integrated procedure was adopted by LAVECCHIA *et al.* (2012) to reconstruct the seismogenic fault sources of the L'Aquila 2009 seismic sequence. Specifically, the depth-contour lines of each individual fault plane activated during the sequence were drawn following a multistage procedure: (1) plot of the seismicity on narrowly-spaced (width = 2.5 km) vertical cross-sections, oriented nearly perpendicular to the fault strike; (2) draw, for each cross-section, the best fit plane connecting the aftershock volume and the fault trace at the surface; (3) project in map view (with 2-km spacing) the depth points lying on each fault along the trace of each section; and (4) interpolate all the points at the same depth to reconstruct the best fit structure contours.

In this paper, we adopted the same procedure to reconstruct the 3D geometry of the fault segments (coloured areas in Fig. 5) activated during the

Colfiorito 1997 sequence. In Fig. 5, the depth-contour lines of the seismological fault portions activated by the Colfiorito and L'Aquila aftershocks are both reported together with the epicentres of the major events associated with each fault segment. The average geological fault parameters (strike, dip, rake and length) of each identified source are summarised in Table 1, where the average pseudo-focal mechanisms have been calculated. For comparison, we also reported the average focal mechanisms computed considering the $M_L \geq 3.5$ events associated with each source. We set apart the solutions in the Annifo sector for which the magnitude threshold was lowered to $M_L \geq 2.4$ (Sect. 4.2).

5.1. Colfiorito 1997 Source Geometry

The depth contour lines of the Colfiorito 1997 individual sources (Fig. 5A) were reconstructed starting from the fault pattern previously outlined (Fig. 3) and from the eighteen 2-km spaced hypocentral sections, elaborated by CHIARALUCE *et al.* (2003), across the epicentral area. We exploited the accurate hypocentral determinations (computed formal errors of 70, 85, and 120 m, respectively, in latitude, longitude, and depth) in this view.

We identified two major well distinguished individual sources corresponding to two first-order fault segments characterised by a right-stepping en echelon arrangement (Figs. 3A, 5A; Table 1). The northern source coincides with the SW-dipping Mt. Pennino-Mt. Prefoglio segment. It extends along the strike for nearly 18 km and, based on the earthquake distribution, reaches a depth of 10 km with a planar geometry and an average dip of $\sim 50^\circ$ (Table 1). The September 26 mainshocks (M_w 6.0 and M_w 5.7) nucleated on the central part of this fault segment (Figs. 3A, 5A).

The southern source can be subdivided into two segments: the SW-dipping Cesi-San Martino and the Mt. Fema faults. The first extends along the strike for nearly 11 km in the N130° direction and the second for nearly 8 km in the \sim N140° direction (Table 1). The activated depths range from 2 to 7 km for the Cesi-San Martino segment and from 4 km to 6 km for the Mt. Fema one.

Our geometric reconstruction, based on the earthquake depth distribution, suggests that the two

Table 1

Average geological (from field data) and seismological (from earthquake data) parameters of the individual fault segments involved in the Colfiorito 1997 and L'Aquila 2009 seismic sequences

Average parameters of individual fault segments	Colfiorito fault system				L'Aquila fault system			
	1 Mt. Pennino- Mt. Prefoglio	2 Cesi-San Martino	3 Mt Fema	4 Annifo	5 Mt. Gorzano	6 Montereale	7 Paganica- Mt. Stabiata	8 Ocre
Geological fault parameters								
Strike	136	130	142	194	150	128	123	–
Dip	60	52	56	87	60	59	50	–
Rake	–81	–86	–92	177	–81	–91	–97	–
Outcropping length (km)	~18	~11	~8	~7	~28	~25	~24	–
Seismological fault parameters								
Strike ^a	136	123	154	185	144	125	136	334
Dip ^a	51	47	51	83	46	49	61	80
Rake ^a	–80	–91	–82	–9	–95	–100	–106	–76
Activated length (km)	~14	~14	~10	~8	~18	North: ~7 South: ~15	~25	~15
Activated depth range (km)	1–10	2–7	4–6	1–4	6–12	North: 6–9 South: 6–10	1–11	11–16

^a The average focal mechanism attitude (Bingham analysis) has been calculated considering $M \geq 3.5$ events with the exception of the solutions in the Annifo sector, for which the magnitude threshold was lowered to $M \geq 2.4$ (see text for details). Fault numbers relate to the seismogenic sources as labelled in Fig. 5. The related kinematic axes are reported in Table 4

faults converge at a depth of nearly 4 km (see depth contour lines in Fig. 5A). The Cesi-S. Martino segment can be associated with the October 3 and 6, 1997, events (M_w 5.2 and M_w 5.4, respectively) located at its northern tip and to the October 14 event (M_w 5.6) located at its southern fault tip, close to the step-over with the Mt. Fema segment. Conversely, the October 12 event (M_w 5.2) is possibly located at the northernmost termination of the Mt. Fema fault.

Whereas the depth distribution of the major events and of most of the associated seismicity fits well with the down-dip projection of the SW-dipping fault segments, a subordinate and localised group of events defines a narrow subvertical volume. It is elongated for ~8 km along the tight N–S Annifo extensional basin and confined to a depth shallower than 4–5 km within the hanging wall of the Cesi fault. The Annifo seismicity, which culminated with the October 16 earthquake (M_L 4.5), was interpreted by CHIARALUCE *et al.* (2004, 2005) as associated with a N–S oriented left-lateral strike-slip fault reactivating a preexisting Late Miocene transcurrent fault, which caused the segmentation and displacement of the Mt. Pennino–Mt. Prefoglio normal fault. Our

structural and kinematic analysis points to another interpretation, which is further discussed.

5.2. L'Aquila 2009 Source Geometry

The depth contour lines of the L'Aquila 2009 individual sources (Fig. 5A) were reconstructed by LAVECCHIA *et al.* (2012), as previously mentioned, starting from the hypocentral location provided in CHIARALUCE *et al.* (2011a) (formal errors ERH-ERZ <1 km). The L'Aquila seismic sequence reactivated four very distinct fault sources differing in their geometry, size, and degree of involvement (LAVECCHIA *et al.* 2012) (Figs. 3B, 5B; Table 1). In order of importance, these sources may be ranked as follows: (1) the SSW to SW-dipping Paganica-Mt. Stabiata fault system, activated during the April 6 mainshock (M_w 6.1) from the surface to a depth of ~11 km; (2) the NE-dipping hidden Ocre source, activated during the strongest aftershock (April 9, M_w 5.4) at depths between 11 and 16 km; (3) the WSW-dipping Mt. Gorzano fault, activated by four relevant aftershocks (April 6–13, $4.8 \leq M_w \leq 5.2$) at depths between 6 and 12 km; and (4) the WSW-dipping Montereale

fault system and its continuation into the S-dipping Mt. San Franco fault, activated at a 6–10 km depth during a large number of minor events with M_w up to 3.5.

The hypocentre of the April 6 main event is sited at a depth of ~ 9 km close to the intersection line between the SW-dipping Paganica fault and the S-dipping Mt. Stabiata fault (see LAVECCHIA *et al.* 2012 for more details), suggesting that the fault plane complexities (in this case, the sharp bend in the fault) represent favourable sites for earthquake nucleation (Fig. 3B), as already highlighted in other seismotectonic settings (KING and NÁBĚLEK, 1985 and references therein).

Most of the authors agree with the activation of the Paganica and Mt. Gorzano SW-dipping faults as the primary-seismogenic sources of the April 6 and 9 events, respectively (ATZORI *et al.* 2009; CHIARABBA *et al.* 2009; LAVECCHIA *et al.* 2011a, b, 2012; CHIARALUCE *et al.* 2011a, b). However, the buried source responsible for the April 7 event (M_w 5.4) is not clearly interpreted. Based on its aftershock sequence, the seismogenic plane appears to dip north-eastward; therefore, some authors suggest the activation of an extensional structure antithetic to the Paganica master fault (PINO and DI LUCCIO 2009, CHIARALUCE *et al.* 2011a, b; VALOROSO *et al.* 2013). Conversely, LAVECCHIA *et al.* (2012) interpreted the entire sequence in a more regional framework, advancing the hypothesis that an east-dipping seismogenic basal detachment, bounding the west-dipping active faults downward, might have been activated by the April 7 event.

6. Colfiorito 1997 and L'Aquila 2009 Source Kinematics

The kinematics of the investigated fault segments was analysed starting from the focal solutions for the $M \geq 2.7$ events computed in CHIARALUCE *et al.* (2004) for the Colfiorito sector and in HERRMANN *et al.* (2011) (the latter integrated up to October 2011 with data available at <http://www.eas.slu.edu/eqc/eqcmt.html>) for the L'Aquila one (Fig. 6A, B). To highlight and schematize the kinematic features of the seismic

sequence, we followed the FROHLICH (1992) classification scheme based on the plunge of the T-, B- and P-axes. The solutions were subdivided into kinematic categories (thrust, thrust-strike, strike-slip, normal, normal-strike and unknown) and represented in a ternary diagram. We also investigated the depth distribution of the focal solutions with the aim to detect seismicity clusters, if any, connected to structural complexities.

6.1. Colfiorito Source Kinematics

The kinematic analysis was based on 162 selected focal mechanisms with $2.7 \leq M_L \leq 5.8$ in the time interval September 3–October 28, 1997 (Fig. 6A). The deformation pattern is not only characterized by normal fault solutions, as is the case for the mainshocks (see details on focal mechanisms in Fig. 2A), but the overall kinematics appears to be of a mixed type.

Most of the Colfiorito focal mechanisms (78 %) plotted on the ternary diagram (FROHLICH 1992) show normal fault and normal oblique solutions (Fig. 6A1). They include the mainshocks (bold focal mechanisms) and aftershocks with higher magnitudes (Fig. 6A) clearly related to the main west-dipping segments of the Colfiorito fault system (BONCIO *et al.* 2000; CHIARALUCE *et al.* 2003, 2005). They also show a prevalent depth distribution between 2 km and 6 km (Fig. 6A2), with a peak concentration at approximately 3 km.

Less than 6 % of the focal mechanisms are represented by reverse (red) or reverse oblique fault mechanisms (yellow); they correspond to events that are not clustered and do not identify any clear structure.

A considerable percentage (14 %) of solutions is represented by strike-slip events (green), which are spatially concentrated in the Annifo sector (upper right inset in Fig. 6A) along the N–S striking seismicity clusters and at depths between 2 km and 4 km (Fig. 6A3).

To investigate further the prevailing kinematics in this small Annifo sector, we lowered the magnitude threshold considering a selected subset of 78 $M_L \geq 2.4$ events located within the boundary of the

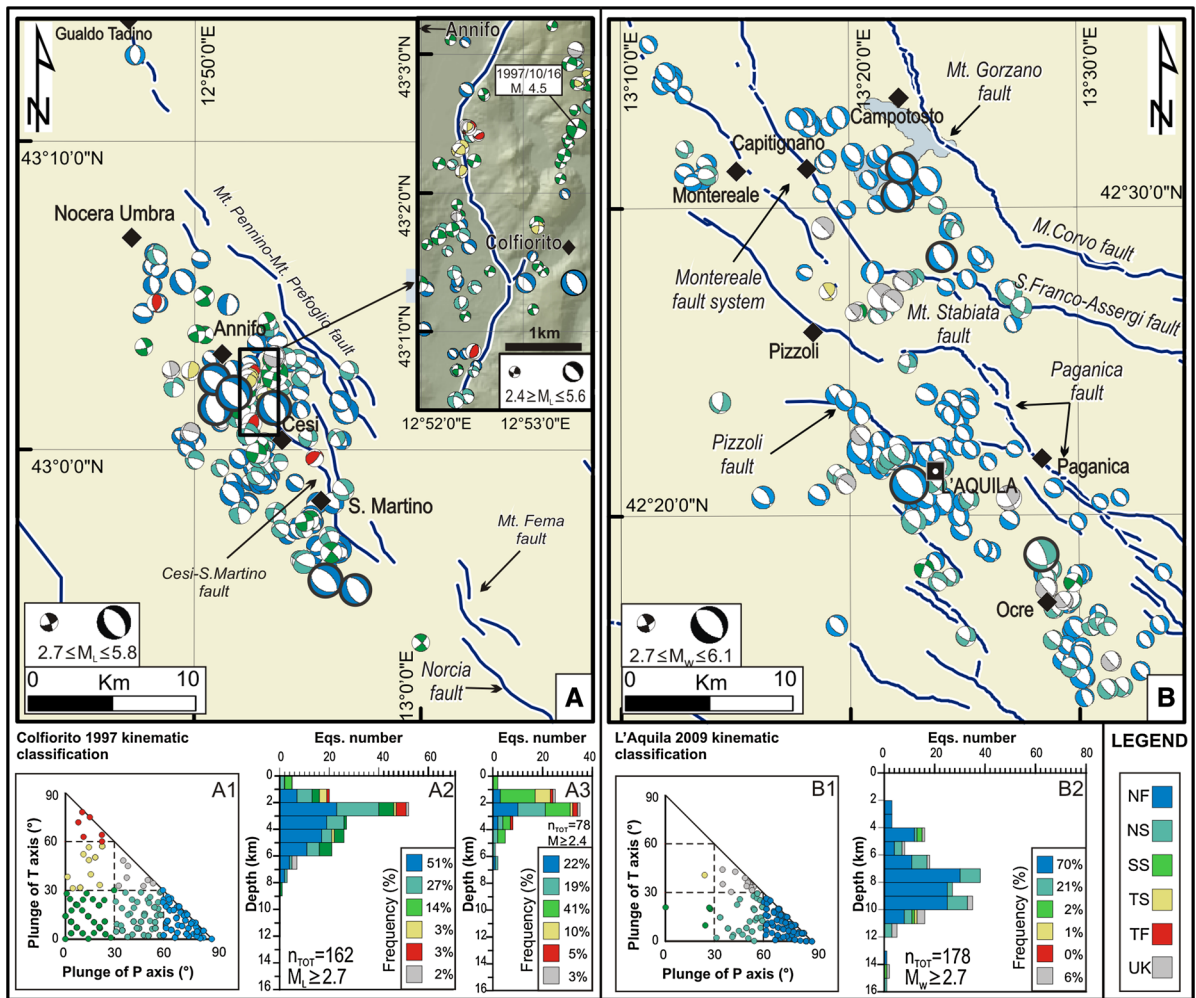


Figure 6

Fault plane solutions used for the kinematics analysis of the Colfiorito 1997 and L'Aquila 2009 seismic sequences (from CHIARALUCE *et al.* 2004; HERMANN *et al.* 2011, respectively). The *upper right lateral inset* in **A** represents the Annifo area with the prevalent strike-slip kinematics at shallower depths. *Different colours* refer to the kinematic classification as derived from the FRÖHLICH (1992) diagram based on the plunge of the T-P axes (*insets A1* in **A** and *B1* in **B**). Key: NF Normal fault, NS normal-strike fault, SS strike slip, TS thrust-strike fault, TF thrust fault, UK unknown kinematics. The histograms in the *insets A2*, *A3* and *B2* of **A** and **B**, respectively, report the frequency of focal mechanisms (for each kinematic group) versus depth

black rectangle delimited in Fig. 6A (approximately 2 km wide and 6 km long). In this area, the frequency of normal faulting solutions falls to 22 %, whereas the strike-slip solutions (including transtensive and transpressive) increases up to a total of 71 %, with a maximum concentration between 1 km and 4 km (Fig. 6A3).

The remaining percentage (8 %) of focal solutions (reverse plus unknown type) also appears to be scattered in the Annifo sector and not clearly related to any structural discontinuity.

6.2. L'Aquila Source Kinematics

The focal mechanisms [178 events with $2.7 \leq M_w \leq 6.1$ in the time interval March 30, 2009–October 30, 2011 (Fig. 6A)] show an absolute prevalence of normal fault solutions (Fig. 6B, B1) for both the mainshocks and the aftershocks (see focal mechanism details in Fig. 2B). They are well represented (70 % frequency) and related to the activation of the Paganica, Mt. Gorzano, and Montereale west-dipping faults (ATZORI *et al.* 2009; CHIARABBA *et al.*

2009; LAVECCHIA *et al.* 2011a, b, 2012; CHIARALUCE *et al.* 2011a, b). The normal fault solutions spread homogeneously between 2 km and 11 km (Fig. 6B2) with a maximum frequency in the 7–9 km depth interval. The ternary diagram (Fig. 6B1) also shows 21 % normal-strike solutions. This group of focal mechanisms includes the April 7, M_w 5.4 mainshock, which struck the Ocre area, and a few events located between 13 km and 16 km (Fig. 6B2) that we associate with an east-dipping extensional detachment in agreement with LAVECCHIA *et al.* (2012).

On the whole, the normal and normal-strike solutions represent 91 % of the overall kinematics, revealing the substantial extensional character of this sequence.

7. Geological and Seismological Stress Inversion

Independent stress tensor inversions aimed to study the stress field affecting central Italy since the Early Quaternary have been applied to the fault-slip (Figs. 3, 4) and focal mechanism data sets (Fig. 6A, B) following the procedure proposed in DELVAUX and SPERNER (2003) (Win-Tensor software, see Sect. 10).

In the inversion technique, we considered four model parameters: the orientation of the three principal axes of the stress ellipsoid (σ_1 , σ_2 , σ_3) and the stress ratio $\Phi = (\sigma_2 - \sigma_3)/(\sigma_1 - \sigma_3)$. The misfit function to optimize F5, using striated fault planes as input data, is built to (1) minimise the slip deviation (misfit = α) between the observed slip line and resolved shear stress (30° misfit value is not expected to be exceeded) and (2) favour higher shear stress magnitudes $|\tau(i)|$ and lower normal stress magnitudes $|\nu(i)|$ to promote slip on the plane. The function contains three terms and is implemented in a way that it ranges from 0 (optimal misfit) to 360 and is independent from the ratio σ_1/σ_3 . The first term, which minimises α , is represented by the function $f(i) = \sin^2(\alpha(i)/2)$ and is dominant with respect to the others (for details, see DELVAUX and SPERNER 2003).

Using seismological data, the input was represented by both nodal planes for each focal mechanism. Afterwards, the plane that is best explained by the stress tensor, in terms of the smallest

misfit function, is considered as the actual fault plane. After this separation, the final inversion then includes only the focal planes that are best fitted by a uniform stress field (GEPHART and FORSYTH 1984; DELVAUX and BARTH 2010). Conversely, using geological data, the required input is represented by the observed fault plane; this option avoids obtaining higher uncertainties.

In applying the procedure, the data were preliminarily analysed using an improved version of the Right Dihedron method (ANGELIER and MECHLER 1977) to determine the starting model parameters (e.g., the reduced stress tensor). The stress tensor determination is achieved by a 4D grid search inversion involving several runs. In the first step, the tensor derived from the kinematic analysis is rotated around each stress axis within a range of $\pm 45^\circ$ in steps of 5° and the full range of R values (0–1) is checked in steps of 0.25. The parameters that give the lowest value of the optimization function are used as the starting point for the next run. The variability ranges of the rotation angles and the R parameter are reduced step-by-step up to a range of $\pm 5^\circ$ and $\pm 0.1^\circ$, respectively.

During the formal inversion, the same weight value was assigned to each fault (i). In contrast, inverting the seismological data, an exponential weight factor ($10^{w(i)}$) was assigned to the i -th focal mechanism, with the exponent $w(i)$ depending on the magnitude: $w(i) = w_o * M(i)/M_{max}$. We set $w_o = 6.5$ in the Colfiorito case and $w_o = 7.5$ in the L'Aquila one. The different choice of w_o allows accounting for the different maximum observed magnitude in the two data sets ($M_L = 5.8$ and $M_w = 6.1$ in the Colfiorito and L'Aquila cases, respectively).

Uncertainties associated with the four model parameters (σ_1 , σ_2 , σ_3 , Φ) are given in terms of 1σ standard deviations. The quality of the results (QRw) for the geological data (A–E, with A the highest quality and E the lowest) are referred to the parameter QR in the World Stress Map project reported in SPERNER *et al.* (2003), while the quality evaluation of the results for the focal mechanism solutions (QRfm) is referred to the updated ranking system of the World Stress Map released in 2008 (HEIDBACH *et al.* 2010). The results are shown in Fig. 7 and summarized in Table 2.

7.1. Geological Stress Inversion

In the Colfiorito area, we separately inverted the fault-slip data belonging to the west-dipping extensional fault system and those surveyed along the Annifo strike-slip fault. In fact, as discussed in Sect. 3.1, the latter nucleated during the Mio-Pliocene compressional phases affecting the Apennine belt. Therefore, it must be excluded from the Quaternary stress field computation. We use a total number (nt) of 91 slickensided fault planes to calculate the geological stress tensor from the west-dipping Colfiorito fault system (Fig. 7A and Table 2). The results are consistent with a normal fault regime with $\sigma_3 = 048/05 \pm 18.7$ and $\Phi = 0.1 \pm 0.1$. As shown in Fig. 7A, the quality rank of this inversion is QRw = A. Only 11 % of data have been rejected since they were not coherent with the computed stress tensor.

However, the slip data collected along the Annifo fault (nt = 18, Fig. 7A1; Table 2) are consistent with a strike-slip fault regime. The resulting stress tensor, in fact, shows a sub-vertical intermediate stress axis ($\sigma_2 = 035/83 \pm 18.7$) and a shape factor $\Phi = 0.82 \pm 0.35$. As we expected, the stress tensor attitude is consistent with the Mio-Plio compressional regime characterized by a NE–SW trending principal compression axis. The inversion results of B quality rank are due to the number of input data (see SPERNER *et al.* 2003).

The inversion of the slickensided fault planes (nt = 81) in the L'Aquila sector gives, as in the Colfiorito case, a geological stress tensor revealing a normal fault regime with $\sigma_3 = 030/05 \pm 12.4$ and $\Phi = 0.1 \pm 0.08$. Most of the data are consistent with the computed stress tensor and only 6 % of the total data set was rejected. The quality rank of these inversion results is QRw = A (Fig. 7B; Table 2).

7.2. Seismological Stress Inversion

When we inverted the seismological data sets, we only considered focal mechanisms of events with $M \geq 3.5$ (epicentres in Fig. 3) to favour the kinematics of the largest magnitudes earthquakes and, consequently, the major seismogenic sources.

Regarding the Annifo sector, we followed the same criteria used in the kinematic analysis. We lowered the magnitude threshold ($M_L \geq 2.4$) considering all the events falling in the black inset of Figs. 3 and 6, because it includes less energetic events (75 events with $2.4 \leq M_L \leq 3.7$) with only one M_L 4.5 event (on October 16). Moreover, we did not include the September 26 mainshock (M_L 5.6) and the September 3 foreshock (M_L 4.4), which are clearly related to the underlying Mt. Pennino-Mt. Prefoglio seismogenic source (Sect. 5.1), in the Annifo subset.

The Colfiorito seismological stress tensor (Fig. 7C; Table 2), obtained from inverting 36 focal mechanisms (nt = 72 nodal planes), shows a normal fault regime with $\sigma_3 = 053/10 \pm 20.9$. The shape factor is $\Phi = 0.21 \pm 0.22$ and the rank quality is QRfm = A.

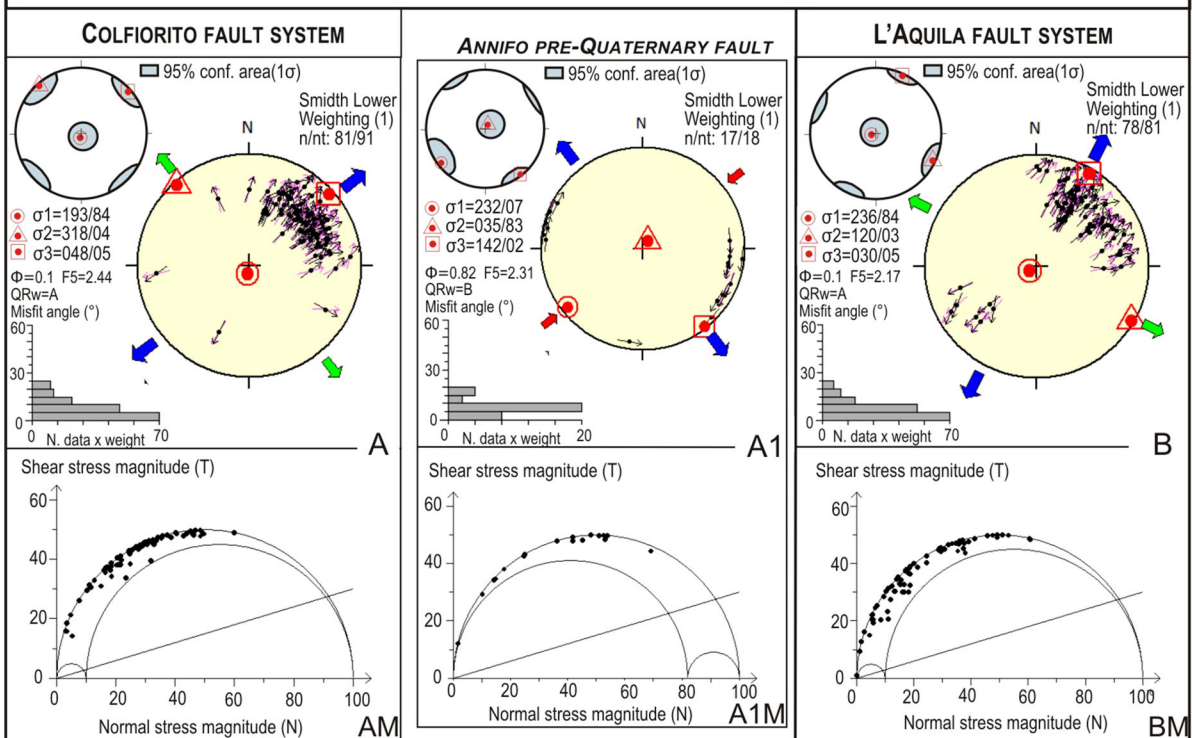
The inversion of the Annifo focal solution subset (nt = 154, Fig. 7C1) highlights a tensor coherent with strike-slip kinematics. The inverted nt = 56 focal mechanisms are, in fact, consistent with a subvertical intermediate axis ($\sigma_2 = 099/81 \pm 15.2$) and a subhorizontal minimum stress ($\sigma_3 = 226/05 \pm 13.7$), and $\Phi = 0.58 \pm 0.33$. Furthermore, the 21 focal mechanisms rejected from the inversion procedure (37 %) were tentatively inverted to detect minor components of the stress tensor. However, the new computation revealed only eight mutually compatible focal mechanisms; this resulted in an unreliable stress tensor attitude.

The inversion of the L'Aquila seismological data set (58 focal mechanisms, nt = 116 nodal planes) shows a stress tensor (Fig. 7D; Table 2) with $\sigma_3 = 048/02 \pm 17.5$, which is nearly coaxial with the one derived from the inversion of the Colfiorito focal mechanisms ($\sigma_3 = 053/10 \pm 20.9$ in Fig. 7C). The shape factor is $\Phi = 0.56 \pm 35$ and the rank quality is QRfm = A.

7.3. Mechanical Analysis of Faulting

To investigate the activation of preexisting discontinuities, we analysed the distribution of the shear stress (T) versus normal stress (N) magnitudes required to produce slip on the analysed faults (variously oriented with respect to the computed stress tensor attitude) on a Mohr diagram. An initial friction angle of 16.7° (BYERLEE 1978) was assumed

FAULT SLIP DATA STRESS INVERSION



FOCAL MECHANISM STRESS INVERSION

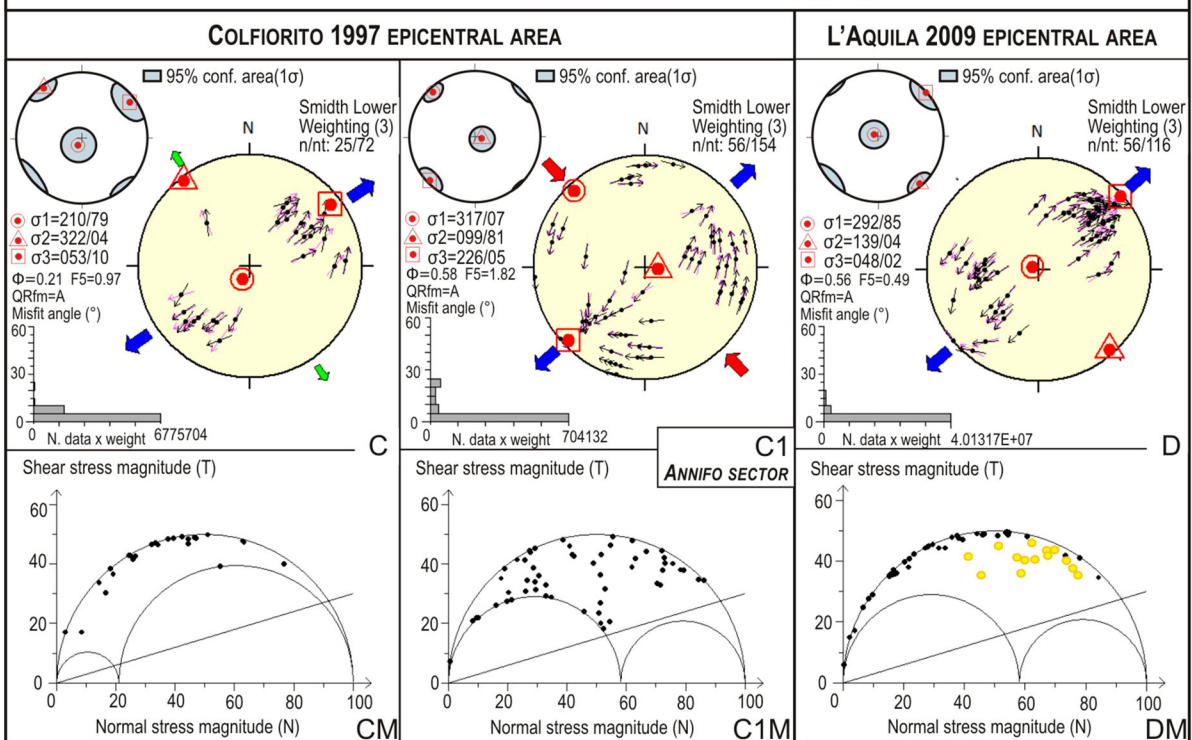


Figure 7

Stress inversion results for the geological (*insets A, AI, B*) and seismological (*insets C, CI, D*) data collected for the two study areas of Colfiorito and L'Aquila (*black and red insets* in Fig. 3). On the lower hemisphere Schmidt nets, the tangent lineations of the fault planes and the selected focal planes are reported; the *dark* and *pink arrows* indicate the measured slip directions and resolved shears, respectively. The attitudes of σ_1 , σ_2 , σ_3 are represented by *red circles, triangles and squares*, respectively. The related maximum and minimum horizontal stress orientations are represented by large arrows outside the stereogram. Their type, length, and colour symbolise the horizontal deviatoric stress magnitude and are a function of the stress regime and the stress ratio $\Phi = (\sigma_2 - \sigma_3)/(\sigma_1 - \sigma_3)$. Key: *blue arrows* when σ_3 is subhorizontal; *green arrows* when σ_2 is subhorizontal; *red arrows* when σ_1 is subhorizontal. *Outward arrows* indicate extensional deviatoric stress, and *inward arrows* indicate compressional deviatoric stress. On the small *upper left nets*, the lower hemisphere projections of the best-fitting principal stress axes (σ_1 , σ_2 , σ_3) and their 95 % confidence area (1σ) are reported. The histograms on the *lower left corner* of the *nets* represent the distribution of the misfit angle α versus the number of data. In the *lower panels* of each data set (*insets AM, AIM, BM, CM, CIM, DM*), the shear stress (T) versus the normal stress (N) magnitude distributions are represented on the respective Mohr diagrams; straight lines represent the initial friction line (friction angle = 16.7°). *Yellow dots* in the *inset DM* represent fault planes reactivated during the L'Aquila 2009 seismic sequence (see details in the text)

and the analysis was performed for the Colfiorito, Annifo, and L'Aquila geological and seismological data sets (Fig. 7 lower panels). We observe that in all the geological cases (Fig. 7AM, AIM, BM), most of the data intersect the largest Mohr circle ($\sigma_1 - \sigma_3$), suggesting the activation of neo-formed fault planes.

Conversely, the Mohr diagrams reconstructed for the focal mechanism data sets (Fig. 7CM, CIM, DM) show a number of the selected preferential planes falling between the largest Mohr circle ($\sigma_1 - \sigma_3$) and

the limiting friction line. This configuration, which reveals the reactivation of preexistent structures, is particularly evident for the Annifo data set (Fig. 7CIM), where the reactivation of an inherited strike-slip fault gave rise to a high percentage of strike-slip focal mechanisms (see upper right inset in Fig. 6A) with sinistral kinematics on N-S oriented planes.

Concerning the L'Aquila data set (Fig. 7D), note that some points falling between the initial friction line and the largest Mohr circle ($\sigma_1 - \sigma_3$) correspond to events localized on the along-strike or along-dip termination lines of the Paganica-Mt. Stabiate, Mont-ereale and Mt. Gorzano sources (yellow circle on the Mohr diagram on Fig. 7DM and yellow bold epicentres in Fig. 5B), or where the main NW-SE trending fault segments intersect the minor E-W-oriented ones. This peculiar behaviour most likely means that the fault portions characterized by structural complexities could represent loci where the stress was focused. We did not observe the same evident behaviour in the Mohr diagram of the Colfiorito subset.

Finally, we exploited the Win-Tensor capability to select the preferential seismogenic plane (i.e., the plane that is best explained by the stress tensor and corresponds to the smaller value of F5) for the focal mechanisms. We note that a coherence is observable between the selected planes and the attitude of the seismogenic sources responsible for the most energetic shocks ($M_L > 5.0$), as constrained by independent geological and seismological interpretations (see Sects. 3 and 4 for details). In fact, in the Colfiorito sector, the preferential seismogenic planes are south west-dipping and NW-SE oriented. Instead, the

Table 2

Stress inversion parameters σ_1 , σ_2 , σ_3 (trend/plunge) and Φ as computed in the inversion procedure of the geological (A, AI, and B) and seismological (C, CI, and D) data sets

Subset	No. of data (inverted/total)	σ_1	$\pm 1\sigma$	σ_2	$\pm 1\sigma$	σ_3	$\pm 1\sigma$	Φ	$(\sigma_2 - \sigma_3)/(\sigma_1 - \sigma_3)$	$\pm 1\sigma$	QR
A—Colfiorito fault system (G)	81/91	193/84	17.8	318/04	19.2	048/05	18.7	0.1		0.1	A
AI—Annifo pre-existing fault (G)	17/18	232/07	21.2	035/83	18.7	142/02	15.2	0.82		0.35	B
B—L'Aquila fault system (G)	78/81	236/84	16.2	120/03	13.3	030/05	12.4	0.1		0.08	A
C—Colfiorito fault system (S)	25/72	210/79	22	322/04	14.4	053/10	20.9	0.21		0.22	A
CI—Annifo re-activated fault (S)	56/154	317/07	10.8	099/81	15.2	226/05	13.7	0.58		0.33	A
D—L'Aquila fault system (S)	56/116	292/85	17.9	139/04	12.7	048/02	17.5	0.56		0.35	A

The uncertainties ($\pm 1\sigma$) associated with the four model parameters and the quality of the results (QR) are also reported (see text for details)

G Geological data, S seismological data

selected planes in the L'Aquila sector dip westwards in the case of the Paganica and Mt. Gorzano mainshocks (April 6, M_w 6.1, and April 9, M_w 5.2, events) and eastwards in the case of the hidden Ocre source (April 7, M_w 5.4); this result possibly gives further constraints to the seismotectonic interpretation proposed in LAVECCHIA *et al.* (2012). The selected preferential planes and the respective computed parameters are summarized in Table 3.

8. Summary of Results and Discussion

The structural-kinematic analysis and the stress inversion of the Colfiorito 1997 and L'Aquila 2009 seismic sequences performed in this paper are based

on the integrated analyses of a large data set of focal mechanisms (CHIARALUCE *et al.* 2004; HERRMANN *et al.* 2011) and fault slip data, most of the latter acquired along major active faults (Figs. 4, 5). In our opinion, the main results, having been derived from independent data, provide additional and more robust constraints to central Italy's local and regional active stress tensor and deformation field. These results are summarized in the following sections.

8.1. Structural Style

The Quaternary faults outcropping in the two study areas highlight an extensional system dominated by individual SW-dipping fault alignments (Figs. 1, 3), prevailinglly arranged in a right-lateral en

Table 3

Nodal planes of the major events ($M_L > 5.0$) of the Colfiorito 1997 and L'Aquila 2009 seismic sequences and kinematic attitude

Colfiorito 1997 major events ($M_L > 5.0$)								
N	Date	M_L	Plane dip dir/dip (°)	Line T/P (°)	Shear T/P (°)	P T/P (°)	B T/P (°)	T T/P (°)
1a	97/09/26	5.8	234/42	221/41	227/42	165/82	317/07	047/04
1b	""	""	041/49	054/48	050/49			
2a	97/09/26	5.6	242/46	232/46	229/45	136/89	327/05	237/01
2b	""	""	052/77	062/44	060/44			
3a	97/10/06	5.4	260/40	247/39	238/38	203/81	342/06	073/06
3b			067/51	080/50	073/51			
4a	97/10/12	5.1	244/51	231/50	228/50	108/81	329/06	238/06
4b	""	""	051/40	064/39	060/40			
5a	97/10/14	5.5	212/38	225/37	219/38	260/79	130/06	039/38
5b	""	""	045/53	032/52	054/53			
L'Aquila 2009 major events ($M_L > 5.0$)								
N	Date	M_L	Plane dip dir/dip (°)	Line T/P (°)	Shear T/P (°)	P T/P (°)	B T/P (°)	T T/P (°)
1a	09/04/06	5.9	225/55	234/55	236/54	025/80	138/04	229/10
1b	""	""	054/35	045/35	046/35			
2a	09/04/07	5.4	070/70	011/54	012/55	288/54	149/28	048/19
2b	""	""	191/36	250/20	224/31			
3a	09/04/09	5.1	235/40	235/40	232/40	235/85	055/05	325/00
3b	""	""	055/50	055/50	043/49			

The preferential (grey rows) and auxiliary seismogenic planes, as selected by the inversion procedure, are highlighted. Keys: Line (T/P) = observed shear (rake) from focal mechanism (Trend/Plunge); shear (T/P) = calculated shear from stress inversion (Trend/Plunge); P, B, T = kinematic axes trends (T) and plunges (P) of each focal mechanism. Fault numbers relate to the seismogenic sources as labelled in Fig. 5

echelon pattern of individual fault segments. Specifically, the Mt. Pennino-Mt. Prefoglio, Cesi-San Martino and Mt. Fema faults outcrop across the Colfiorito epicentral area for a total length of ~ 35 km (Figs. 2A, 3), whereas the Mt. Gorzano, Montereale and Mt. Stabiata-Paganica faults extend for a total length of ~ 50 km (Figs. 2B, 3). The geometry and segmentation pattern are typical of Quaternary normal and normal-oblique faults from the northern-central Apennines (GALADINI and GALLI 2000; LAVECCHIA *et al.* 2002; BONCIO *et al.* 2000, 2004; BROZZETTI *et al.* 2009).

8.2. Active Fault Kinematics

The kinematics of the Quaternary fault system constrained by the geological-structural data discussed in the text (nearly 250 of the fault-slip data, Fig. 4) is extensional, characterized by normal and normal-oblique faults (Figs. 3, 4). In fact, the strike-slip deformation surveyed along the N–S Annifo sector shows a right-lateral sense of shear, compatible with the preexisting late-Miocene compressional regime. At all scales, the surface deformation pattern is purely extensional and does not fit with the strike-slip model proposed by previous investigators (CELLO *et al.* 1997; ELTER *et al.* 2012; D'AMICO *et al.* 2013).

8.3. Earthquake Kinematics

The kinematics of the seismogenic deformation, as inferred from the focal mechanism analysis (340 fault plane solutions for $M \geq 2.7$ events), is almost purely extensional in the L'Aquila area, whereas it is slightly more complex in the Colfiorito one (Fig. 6). Nearly 90 % of the L'Aquila events show normal and normal oblique solutions (Fig. 6B2). Conversely, in the Colfiorito area, although the extensional component prevails (78 %), the strike-slip one cannot be neglected (14 % of the data in Fig. 6A2). However, the spatial distribution of the strike-slip focal mechanisms suggests that this component has no regional tectonic meaning because it is not homogeneously spread over the entire epicentral area, but it is concentrated in the narrow Annifo strike-slip zone (see the zoom in the upper right inset in Fig. 6A). Here, a preexisting N–S right-lateral structure

inherited from the Mio-Pliocene compressional phase was reactivated at shallow depths. Differently from other interpretations (CHIARALUCE *et al.* 2005; CARAFA and BARBA 2011), we observe that the strike-slip faulting did not play a relevant role in segmenting the Colfiorito seismogenic sources, and the Annifo fault cannot play the role of a deep-seated strike-slip fault both for the shallow signature of the associated seismicity and its limited extent. As a further support for these arguments, we stress that the Annifo fault zone only released low energetic events (M_L up to 3.7 in the time interval September 29–October 28), with only one earthquake having $M_L = 4.5$ (October 26, 1997).

8.4. Stress Field

The geological and seismological stress tensors computed for the L'Aquila and Colfiorito areas (Fig. 7; Table 2) are nearly coaxial with subhorizontal NE–SW directed σ_3 -axes. The same σ_3 -axis attitude is observed even in the case of the Annifo strike-slip seismological data set. After all, permutations of stress axes commonly occur (ANGELIER 1989), with the most frequent switch, in extensional tectonics, being σ_1/σ_2 . This statement fits well with remarks on the Annifo sector.

The computed tensors are similar and differ only in the stress ratio values Φ obtained by inverting the L'Aquila focal mechanisms (Fig. 7; Table 2). In fact, they have low values ($\Phi = 0.1$) and are representative of radial extension, as defined in DELVAUX *et al.* (1995). Regarding the L'Aquila and Annifo seismological inversions (Fig. 7D, C1), the Φ values are higher and indicative of pure extensional ($\Phi = 0.56$) and strike-slip ($\Phi = 0.58$) regimes, respectively. We consider that the low stress ratio observed for the Colfiorito and L'Aquila geological data might suffer from the influence of a relatively wide time window of tectonic activity (at least the entire Quaternary). Instead, the kinematic heterogeneity of the focal mechanism data set (Fig. 6, insets A1, A2) could be the answer for the low stress ratio values obtained in the Colfiorito seismological case. On the other hand, the higher values characterizing the L'Aquila extensional sequence might reflect its evident kinematic homogeneity (Fig. 6, insets B1, B2). Finally, the high

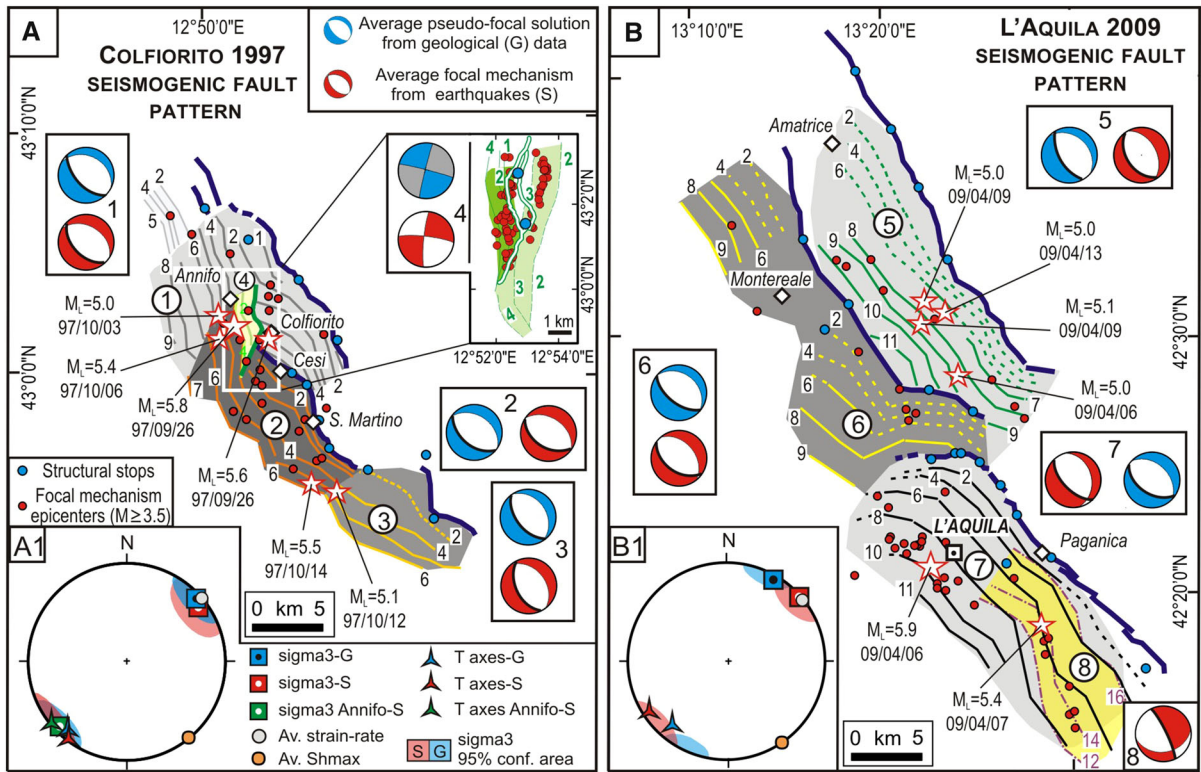


Figure 8

Summary of the kinematic and stress analysis and proposed seismotectonic interpretation for the Colfiorito 1997 (A) and L'Aquila 2009 (B) sectors with schematic seismicogenic sources, depth-contour lines and associated average solutions computed from geological (*blue* pseudo-focal mechanism) and $M \geq 3.5$ earthquake (*red beach ball*) data. **Bold black line**, in the beach balls, represents the preferential seismic plane as computed by stress inversion procedure. Individual source key: 1 Mt. Pennino-Mt. Prefoglio, 2 Cesi-S. Martino, 3 Mt. Fema, 4 Annifo, 5 Mt. Gorzano, 6 Montereale-S. Franco, 7 Paganica-Mt. Stabiata, 8 hidden Ocre. Stars are the epicentres of the $M_L \geq 5.0$ events. *Insets A1* and *B1*: lower hemisphere projections of the geological (*G-blue*) and seismological (*S-red*) T-axes, computed on the whole data sets pertaining the two sectors, and of the least principal stress axes (σ_3) coming from this study with related confidence areas. *Green colour* relates to the Annifo strike-slip source. The average Sh_{max} direction from CARAFA and BARBA (2013) (*orange circle*) and the average principal strain rate axis from DEVOTI et al. (2011) (*grey circle*) are also reported

stress ratio values characterizing the strike-slip deformation of the Annifo source might be related to a deformation context that, in this case, is more confined in time and space. We would like to remark, however, that worldwide and in different tectonic settings, low stress ratio values are more common than high ones (ANGELIER 1984).

8.5. Preferential Seismic Planes

The stress inversion procedure has also allowed us to further constrain the preferential seismic plane of the most energetic events of the two sequences ($M_L > 5.0$). The obtained results (Table 3) ensue from the independent choices performed by the

inversion procedure based exclusively on geometric and mechanical criteria. The stress inversion parameters highlight that the southwest-dipping seismic normal fault planes for all major 1997 Colfiorito events (Fig. 2A) are the preferential ones. These results are in agreement with previous studies following different approaches (BONCIO and LAVECCHIA 2000b; CHIARALUCE et al. 2004, 2005).

In addition, the southwest-dipping seismic normal fault planes are the selected ones for two of the major events of the L'Aquila 2009 sequence (Fig. 2B), which is in agreement with most of the literature. On the contrary, the selected source of the April 7, 2009 event (Fig. 2B) coincides with an east-dipping seismicogenic fault plane, supporting the same results

Table 4

Seismological (S) and Geological (G) kinematic axes (P, B, T) of each fault segment from the L'Aquila and Colfiorito fault systems, as derived from the average focal solutions given in Fig. 8 (Bingham statistics) and from the computation of an average pseudo-focal mechanism from the fault-slip data

Seismogenic sources	P T/P (°)	B T/P (°)	T T/P (°)
Colfiorito fault system			
1 Mt. Pennino-Mt. Prefoglio-S	96/81	310/08	219/05
Mt. Pennino-Mt. Prefoglio-G	69/74	312/08	220/14
2 Cesi-S.Martino-S	06/87	124/01	214/02
Cesi-S.Martino-G	57/82	309/02	219/08
3 Mt. Fema-S	106/82	329/06	238/06
Mt. Fema-G	53/82	320/00	230/09
4 Annifo-S	141/12	328/78	231/01
L'Aquila fault system			
5 Mt. Gorzano-S	331/86	148/04	238/00
Mt. Gorzano-G	79/69	330/07	237/20
6 Montereale-Mt. S. Franco-S	337/82	131/08	222/04
Montereale-Mt. S. Franco-G	40/76	134/01	224/14
7 Paganica- Mt. Stabiata-S	11/70	144/14	238/14
Paganica- Mt. Stabiata-G	21/72	122/04	213/18
8 Ocre-S	277/46	148/32	39/27

Fault numbers relate to the seismogenic sources as labelled in Fig. 5. Keys: (T/P) = trend/plunge

provided by PINO and DI LUCCIO (2009), CHIARALUCE *et al.* (2011a, b), LAVECCHIA *et al.* (2012) and VALOROSO *et al.* (2013).

Moreover, the distribution of the shear stress (T) versus the normal stress (N) magnitudes required to produce slip on the analysed faults (Mohr circles in Fig. 7, lower panels) also suggests a possible distinction between neo-formed and reactivated fractures. The first was generated under the Quaternary extensional stress field, as was the case in the Colfiorito (Fig. 7AM) and L'Aquila fault systems (Fig. 7BM); the second possibly reactivated preexisting contractional strike-slip faults, as in the Annifo case (Fig. 7C1M).

8.6. Comparison Between Geological and Seismological Deformation

The kinematic and stress analysis (Figs. 6, 7) performed in the Colfiorito and L'Aquila areas gives us a chance to compare the attitude of the long-term (e.g., Quaternary) and the present-day seismogenic deformations in central Italy. To this end, we represent in Fig. 8A, B the average focal solutions

computed starting from fault-slip (blue pseudo-focal mechanisms) and earthquakes (red beach ball) associated with the individual sources and discussed in the previous sections. We highlight the preferential seismic plane as computed by stress inversion procedure (bold black line in Fig. 8; Table 3). We also project the attitudes of the geological (G) and seismological (S) T-axes averaged over the whole data sets (Bingham statistics, BINGHAM 1974—all kinematic axes are reported in Table 4) and of the least-principal stress computed in this study (lower hemisphere Schmidt nets in Fig. 8A1, B1).

In both the Colfiorito and L'Aquila cases, a prevailing pure extensional regime is evident. A substantial parallelism among the T-axes and σ_3 , all subhorizontal, and NE–SW trending, can also be noted. Seismological and geological data cannot be directly compared in the Annifo case since the geological pseudo-focal mechanisms (grey beach ball) do not refer to the Quaternary kinematics but rather to the Late Miocene compressional phase (see Sects. 3.1 and 5.1). Nevertheless, the NE–SW trends of the seismological T-axes highlight a likely reactivation of this fault segment during the 1997 seismic sequence with inverted kinematics. A slight strike-slip component was also obtained in the case of the Paganica-Mt. Stabiata (7) and, particularly, of the Ocre hidden (8) sources. This kinematics, however, does not affect the extensional direction, which remained subhorizontal and NE–SW trending when considering the whole data sets (Fig. 8B1).

Finally, we note that all our results are coherent with the regional deformational field in central Italy as inferred from the average principal strain rate axis from DEVOTI *et al.* (2011) and when considering the Sh_{max} directions reported in CARAFA and BARBA (2013).

9. Conclusions

The integrated structural-seismological approach followed in this study allowed us to analyse the active geometry, kinematics, and stress field tensor in two areas of the central Apennines that recently

underwent relevant instrumental earthquakes (e.g., the Colfiorito 1997 and L'Aquila 2009 events). A comparison of the stress tensors from focal mechanisms and field data had already been reported in the literature for the Norcia and Colfiorito areas (BROZZETTI and LAVECCHIA 1994; BONCIO and LAVECCHIA 2000a; CELLO *et al.* 1997) but not for the L'Aquila area. In addition, a coherent overview of the stress field orientation over the region, which is also based on a relevant number of field data and on the careful geometric analysis of the earthquake fault association, represents, in our opinion, an original contribution of this paper.

The two seismic sequences and the associated fault systems, extending for a total length of nearly 120 km in the NW–SE direction, cover a large area of the central Apennines and, therefore, may be considered representative of the Quaternary and active deformation field at a regional scale. Although some authors (ELTER *et al.* 2012; CARAFA and BARBA 2011; D'AMICO *et al.* 2013), also in line with part of the previous literature (CELLO *et al.* 1997), advanced a hypothesis of the important role of strike-slip tectonics at the regional scale, our results point to a completely different scenario, showing the persistence of a constant SW–NE trending tensional stress regime in the Umbria-Marche-Abruzzi region, at least since the Early Quaternary. This evidently does not exclude the possibility of very local and minor reactivations of preexisting faults with strike-slip kinematics.

10. Data and Resources

Kinematic analysis was performed using the FaultKin software by R. ALLMENDIGER (2011) available at <http://www.geo.cornell.edu/geology/faculty/RWA/programs/faultkin-5-beta.html>.

Some figures were created using the GMT package by P. WESSEL and W.H.F. SMITH, available at <http://gmt.soest.hawaii.edu/>.

Some focal mechanisms cited in Fig. 1 are from Harvard CMT database at <http://www.globalcmt.org/CMTsearch.html>.

Win-Tensor, Vers. 4.0 by D. DELVAUX (2011) is available at <http://www.damiendelvaux.be/Tensor/WinTensor/win-tensor.html>.

Acknowledgments

This work was financed by DiS.P.U.Ter, Ud'A University of Chieti (research funds to Giusy Lavecchia). We thank the Editor Yehuda Ben-Zion, the reviewer Salvatore Barba, and the anonymous reviewer for the useful and constructive comments that helped to improve the original manuscript.

REFERENCES

- AMORUSO, A., CRESCENTINI, L., and SCARPA, R. (1998), *Inversion of source parameters from near- and far-field observations: an application to the 1915 Fucino earthquake, central Apennines, Italy*. *J. Geophys. Res.*, *103*, 29989–29999.
- ANGELIER, J. (1984), *Tectonic analysis of fault slip data sets*. *Geophys. Res.*, *89*, 5835–5848.
- ANGELIER, J., and MECHLER, P. (1977), *Sur une méthode graphique de recherche des contraintes principales également utilisable en tectonique et en sismologie : la méthode des dièdres droits*. *B. Soc. Géol. Fr.*, *7*, 1309–1318.
- ANGELIER, J. (1989), *From orientation to magnitudes in paleostress determinations using fault slip data*, *J. Struct. Geol.*, *11*, 37–50.
- ANZIDEI, M., BOSCHI, E., CANNELLI, V., DEVOTI, R., ESPOSITO, A., GALVANI, A., MELINI, D., PIETRANTONIO, G., RIGUZZI, F., SEPE, V., and SERPELLONI, E. (2009), *Coseismic deformation of the destructive April 6, 2009 L'Aquila earthquake (central Italy) from GPS data*, *Geophys. Res. Lett.*, *36*, L17307, doi:10.1029/2009GL039145.
- ATZORI, S., HUNSTAD, I., CHINI, M., SALVI, S., TOLOMEI, C., BIGNAMI, C., STRAMONDO, S., TRASATTI, E., ANTONIOLI, A., and BOSCHI, E. (2009), *Finite fault inversion of DInSAR coseismic displacement of the 2009 L'Aquila earthquake (central Italy)*, *Geophys. Res. Lett.*, doi:10.1029/2009GL039293.
- BARBA, S. and BASILI, R. (2000), *Analysis of seismological and geological observation for moderate-size earthquakes: the Colfiorito Fault System (Central Apennines, Italy)*, *Geophys. J. Int.*, *141*, 241–252.
- BARBA, S., CARAFA, M.M.C., and BOSCHI, E. (2008), *Experimental evidence for mantle drag in the Mediterranean.*, *Geophys. Res. Lett.*, *35*, L06302.
- BARCHI, M., and MIRABELLA, F. (2009), *The 1997–98 Umbria–Marche earthquake sequence: “Geological” vs. “seismological” faults*, *Tectonophysics*, *476*, 170–179.
- BASILI, R., BOSI, V., GALADINI, F., GALLI, P., MEGHRAOUI, M., MESSINA, P., MORO, M., and SPOSATO, A. (1998), *The Colfiorito earthquake sequence of September–October 1997: surface breaks and seismotectonic implications for the Central Apennines (Italy)*, *J. Earthquake Engineering*, *2*, 291–302.
- BINGHAM, C. (1974), *An antipodally symmetric distribution on the sphere*, *Annals of Statistics*, *2*, 1201–1225.
- BONCIO, P., BROZZETTI, F., and LAVECCHIA, G. (1996), *State of stress in the northern Umbria-Marche Apennines (central Italy): inferences from microearthquake and fault kinematics analyses*, *Annales Tectonicae*, *10*, 80–97.
- BONCIO, P., and LAVECCHIA, G. (2000a), *A structural model for active extension in Central Italy*, *J. Geod.*, *29*, 233–244.

- BONCIO, P., and LAVECCHIA, G. (2000b), *A geological model for the Colfiorito earthquakes (September-October 1997, central Italy)*, J. Seismol., 4, 345–356.
- BONCIO, P., BROZZETTI, F., and LAVECCHIA, G. (2000), *Architecture and seismotectonics of a regional low-angle normal fault zone in central Italy*, Tectonics, 19, 1038–1055.
- BONCIO, P., LAVECCHIA, G. and PACE, B. (2004), *Defining a model of 3D seismogenic sources for Seismic Hazard Assessment applications: the case of central Apennines (Italy)*, J. Seismol., 8, 407–425.
- BONCIO, P., PIZZI, A., BROZZETTI, F., POMPOSO, G., LAVECCHIA, G., DI NACCIO, D., and FERRARINI, F. (2010), *Coseismic ground deformation of the 6 April 2009 L'Aquila earthquake (central Italy, Mw 6.3)*, Geophys. Res. Lett., 37, L06308, doi:10.1029/2010GL042807.
- BROZZETTI, F., and LAVECCHIA, G. (1994), *Seismicity and related extensional stress field: the case of the Norcia Seismic Zone (Central Italy)*, Annales Tectonicae, 8, 36–57.
- BROZZETTI, F., BONCIO, P., LAVECCHIA, G., and PACE, B. (2009), *Present activity and seismogenic potential of a low-angle normal fault system (Città di Castello, Italy): Constraints from surface geology, seismic reflection data and seismicity*, Tectonophysics, 463, 31–46.
- BYERLEE, J.D. (1978), *Friction of rocks*, Pure and Applied Geophysics, 116, 615–626.
- CALAMITA, F., and PIZZI, A. (1994), *Recent and active extensional tectonics in the southern Umbro-Marchean Apennines (Central Italy)*, Memorie Società Geologica Italiana, 48, 541–548.
- CALAMITA, F., COLTORTI, M., PIERANTONI, P.P., PIZZI, A., SCISCIANI, V., and TURCO, E. (1999), *Relazioni tra le faglie quaternarie e la sismicità nella dorsale Appenninica umbro-marchigiana: L'area di Colfiorito*, Studi Geologici Camerti, 14, 177–191.
- CARAFÀ, M.M.C., and BARBA, S. (2011), *Determining rheology from deformation data: The case of central Italy*, Tectonics, 30, TC2003, doi:10.1029/2010TC002680.
- CARAFÀ, M.M.C., and BARBA, S. (2013), *The stress field in Europe: optimal orientations with confidence limits*, Geophys. J. Int., doi: 10.1093/gji/ggt024.
- CELLO, G., DEIANA, G., FERELLI, L., MARCHEGIANI, L., MASCHIO, L., MAZZOLI, S., MICETTI, A., SERVA, L., TONDI, E. and VITTORI, T. (2000), *Geological constraints for earthquake faulting studies in the Colfiorito area (central Italy)*, J. Seismol., 4, 357–364.
- CELLO, G., MAZZOLI, S., TONDI, E., and TURCO E. (1997), *Active tectonics in the central Apennines and possible implications for seismic hazard analysis in peninsular Italy*, Tectonophysics, 272, 43–68.
- CHIARABBA, C., AMATO, A., ANSELMINI, M., BACCESCHI, P., BIANCHI, I., CATTANEO, M., CECERE, G., CHIARALUCE, L., CIACCIO, M.G., DE GORI, P., DE LUCA, G., DI BONA, M., DI STEFANO, R., FAENZA, L., GOVONI, A., IMPROTA, L., LUCENTE, F.P., MARCHETTI, A., MARGHERITI, L., MELE, F., MICHELINI, A., MONACHESI, G., MORETTI, M., PASTORI, M., PIANA AGOSTINETTI N., PICCININI, D., ROSELLI, P., SECCIA, D. and VALOROSO, L. (2009), *The 2009 L'Aquila (central Italy) M_w 6.3 earthquake: Mainshock and aftershocks*, Geophys. Res. Lett., 36, L18308, doi:10.1029/2009GL039627.
- CHIARALUCE, L., AMATO, A., COCCO, M., CHIARABBA, C., SELVAGGI, G., DI BONA, M., PICCININI, D., DESCHAMPS, A., MARGHERITI, L., COURBOULEX, F., and RIFEPE, M. (2004), *Complex normal faulting in the Apennines thrust-and-fold belt: The 1997 seismic sequence in central Italy*, Bull. Seismol. Soc. Amer., 94, 99–116.
- CHIARALUCE, L., BARCHI, M., COLLETTINI, C., MIRABELLA, F. and PUCCI, S. (2005), *Connecting seismically active normal faults with Quaternary geological structures in a complex extensional environment: The Colfiorito 1997 case history (northern Apennines, Italy)*, Tectonics, 24, TC1002, doi:10.1029/2004TC001627.
- CHIARALUCE, L., CHIARABBA, C., DE GORI, P., DI STEFANO, R., IMPROTA, L., PICCININI, D., SCHLAGENHAUF, A., TRAVERSA, P., VALOROSO, L., and VOISIN, C. (2011a), *The 2009 L'Aquila (central Italy) seismic sequence*, B. Geofis. Teor. Appl., 52, 367–387.
- CHIARALUCE, L., VALOROSO, L., PICCININI, D., DI STEFANO, R., DE GORI, P. (2011b), *The anatomy of the 2009 L'Aquila normal fault system (central Italy) imaged by high resolution foreshock and aftershock locations*, J. Geophys. Res., B: Solid Earth, 116, B12311, doi:10.1029/2011JB008352.
- CHIARALUCE, L., ELLSWORTH, W.L., CHIARABBA, C., and COCCO, M. (2003), *Imaging the complexity of an active normal fault system: The 1997 Colfiorito (central Italy) case study*, J. Geophys. Res., B: Solid Earth, 108, 1–19.
- CIACCIO, M.G., BARCHI, M.R., CHIARABBA, C., MIRABELLA, F., and STUCCHI, E. (2005), *Seismological, geological and geophysical constraints for the Gualdo Tadino fault, Umbria-Marche Apennines (central Italy)*, Tectonophysics, 406, 233–247.
- CINTI, F.R., CUCCI, L., MARRA, F., and MONTONE, P. (1999), *The 1997 Umbria-Marche (Italy) earthquake sequence: Relationship between ground deformation and seismogenic structure*, Geophys. Res. Lett., 26, 895–898.
- CINTI, F.R., PANTOST, I.D., DE MARTINI, P.M., PUCCI, S., CIVICO, R., PIERDOMINICI, S., CUCCI, L., BRUNORI, C.A., PINZI, S. and PATERA, A. (2011), *Evidence for surface faulting events along the Pagana fault prior to the 6 April 2009 L'Aquila earthquake (central Italy)*, J. Geophys. Res., 116, B07308, doi:10.1029/2010JB007988.
- CIRELLA, A., PIATANESI, A., COCCO, M., TINTI, E., SCOGNAMIGLIO, L., MICHELINI, A., LOMAX A. and BOSCHI E. (2009), *Rupture history of the 2009 L'Aquila (Italy) earthquake from non-linear joint inversion of strong motion and GPS data*, Geophys. Res. Lett., 36, L19304, doi:10.1029/2009GL039795.
- D'AMICO, S., ORECCHIO, B., PRESTI D., NERI, G., WU, W., SANDU, I., ZHU, L., and HERRMANN, R.B. (2013), *Source parameters of small and moderate earthquakes in the area of the 2009 L'Aquila earthquake sequence (central Italy)*, Phys. Chem. Earth, doi:10.1016/j.pce.2013.02.005.
- D'AGOSTINO, N., MANTENUTO, S., D'ANASTASIO, E., AVALLONE, A., BARCHI, M., COLLETTINI, C., RADICIONI, F., STOPPINI, A., and FASTELLINI, G. (2009), *Contemporary crustal extension in the Umbria-Marche Apennines from regional CGPS networks and comparison between geodetic and seismic deformation*, Tectonophysics, 476, 3–12.
- DEIANA, G., and PIALLI, G., (1994), *The structural provinces of the Umbro-Marchean Apennines*, Mem. Soc. Geol. It., 48, 473–484.
- DELVAUX, D., and BARTH, A. (2010), *African stress pattern from formal inversion of focal mechanism data*, Tectonophysics, 482, 105–128.
- DELVAUX, D., and SPERNER, B. (2003), *New aspects of tectonic stress inversion with reference to the TENSOR program*. In: NIEUWLAND, D. A. (ed.) *New Insights into Structural Interpretation and Modelling*, J. Geol. Soc. London, Special Publications, 212, 75–100.
- DELVAUX, D., MOEYS, R., STAPEL, G., MELNIKOV, A., and ERMIKOV V. (1995), *Palaeostress reconstructions and geodynamics of the*

- Baikal region, Central Asia, Part I. Palaeozoic and Mesozoic pre-rift Evolution*, Tectonophysics, 252, 61–101.
- DEVOTI, R., ESPOSITO, A., PIETRANTONIO, G., PISANI, A. R., and RIGUZZI, F. (2011), *Evidence of large scale deformation patterns from GPS data in the Italian subduction boundary*, Earth Planet. Sci. Lett., 311, 230–241.
- DISS WORKING GROUP (2010). Database of Individual Seismogenic Sources (DISS), Version 3.1.1: A compilation of potential sources for earthquakes larger than M 5.5 in Italy and surrounding areas, Available at <http://diss.rm.ingv.it/diss/>, doi:10.6092/INGV.IT-DISS3.1.1.
- EKSTRÖM, G., MORELLI, A., BOSCHI, E., and DZIEWONSKI A.M. (1998), *Moment tensor analysis of the Central Italy Earthquake Sequence of September–October 1997*. Geophys. Res. Lett., 25, 1971–1974.
- ELTER, F.M., ELTER, P., EVA, C., KRAUS, R.K., PADOVANO, M., and SOLARINO, S. (2012). *An alternative model for the recent evolution of the Northern-Central*. J. Geodyn., 54, 55–63.
- EMERGOE WORKING GROUP. (2009), *Evidence for surface rupture associated with the Mw 6.3 L'Aquila earthquake sequence of April 2009 (central Italy)*, Terra Nova, 00, 1–9.
- FALCUCCI, E., GORI, S., PERONACE, E., FUBELLI, G., MORO, M., SAROLI, M., GIACCIO, B., MESSINA, P., NASO, G., SCARDIA, G., SPOSATO, A., VOLTAGGIO, M., GALLI, P., and GALADINI, F. (2009). *The Paگانica fault and surface coseismic ruptures caused by the 6 April 2009 earthquake (L'Aquila, Central Italy)*, Seismol. Res. Lett., 80, 940–950.
- FERRARINI, F., LAVECCHIA, G., de NARDIS, R., and ROMANO, M.A. (2013). *Active deformation field from earthquakes and faults in the Colfiorito 1997 and L'Aquila 2009 seismic sequence epicentral areas (central Italy)*, Rend. Soc. Geol. It., 29, 51–54.
- FROHLICH, C., (1992), *Triangle diagrams: ternary graphs to display similarity and diversity of earthquake focal mechanisms*, Phys. Earth Planet. Inter., 75, 193–198.
- GALADINI, F., and GALLI, P. (2000), *Active tectonics in the Central Apennines (Italy)-Input data for Seismic Hazard Assessment*, Nat. Hazards, 22, 225–270.
- GALLI, P., and GALADINI, F. (1999), *Seismotectonic framework of the 1997-1998 Umbria-Marche (central Italy) earthquakes*, Seismol. Res. Lett., 70, 417–427.
- GALLI, P., GIACCIO, B. and MESSINA P. (2010), *The 2009 central Italy earthquake seen through 0.5 Myr-long tectonic history of the L'Aquila faults system*, Quaternary Sci. Rev., 29, 3768–3789.
- GALVANI, A., ANZIDEI, M., DEVOTI, R., ESPOSITO A., PIETRANTONIO G., PISANI, A. R., RIGUZZI, F., SERPELLONI, E. (2012), *The interseismic velocity field of the central Apennines from a dense GPS network*, B. Geofis. Teor. Appl., 55, doi:10.4401/ag-5634.
- GEHART, J.W., and FORSYTH, D.W. (1984), *An improved method for determining the regional stress tensor using earthquake focal mechanism data: application to the San Fernando earthquake sequence*, J. Geophys. Res., 89, 9305–9320.
- GUIDOBONI, E., FERRARI, G., MARIOTTI, D., COMASTRI, A., TARABUSI, G. and VALENSISE, G. (2007), CFTI4Med, Catalogue of Strong Earthquakes in Italy (461 B.C.-1997) and Mediterranean Area (760 B.C.-1500), INGV-SGA, <http://storing.ingv.it/cfti4med/>.
- HEIDBACH, O., TINGAY, M., BARTH, A., REINECKER, J., KURFEß, D., and MÜLLER, B. (2010). *Global crustal stress pattern based on the World Stress Map database release 2008*, Tectonophysics, 482, 3–15.
- HERRMANN, R.B., MALAGNINI, L., and MUNAFÒ, I. (2011), *Regional Moment Tensors of the 2009 L'Aquila Earthquake Sequence*, Bull. Seismol. Soc. Am., 101, 975–993, doi:10.1785/0120100184.
- HUNSTAD, I., SELVAGGI, G., D'AGOSTINO, N., ENGLAND, P., CLARKE, P. and PIEROZZI M. (2003), *Geodetic strain in peninsular Italy between 1875 and 2001*, Geophys. Res. Lett., 30, 1181, doi:10.1029/2002GL016447.
- KING, G., and NÁBĚLEK, J. (1985), *Role of fault bends in the initiation and termination of earthquake rupture*, Science, 228, 984–987.
- LAVECCHIA, G. (1988). *The Tyrrhenian-Apennines system: structural setting and seismotectogenesis*, Tectonophysics, 147, 263–296.
- LAVECCHIA, G., BONCIO, P., BROZZETTI, F., DE NARDIS, R., DI NACCIO, D., FERRARINI, F., PIZZI, A., and POMOSO, G. (2011a), *The April 2009 L'Aquila (Central Italy) seismic sequence (M_w 6.3): A Preliminary Seismotectonic Picture*, In Recent Progress on Earthquake Geology (ed. Guarnieri P.) (Nova Science Publishers, New York), 1–17, ISBN/ISSN:978-1-60876-147-0.
- LAVECCHIA, G., BONCIO, P., BROZZETTI, F., DE NARDIS, R., VISINI, F. (2011b), *The contribution of structural geology and regional tectonics to the definition of large-scale seismotectonic provinces and individual seismogenic sources: Application to the extensional belt of central Italy*. In Recent Progress on Earthquake Geology (ed. Guarnieri P.) (Nova Science Publishers, New York), 165–187, ISBN/ISSN:978-1-60876-147-0.
- LAVECCHIA, G., BONCIO, P., BROZZETTI, F., STUCCHI, M. and LESCIIUTTA I. (2002), *New criteria for seismotectonic zoning in Central Italy: insights from the Umbria-Marche Apennines*, Boll. Soc. Geol. It., Spec. V. 1, 881–890.
- LAVECCHIA, G., BROZZETTI, F., BARCHI, M., MENICETTI, M. and KELLER J.V.A. (1994), *Seismotectonic zoning in east-central Italy deduced from an analysis of the Neogene to present deformations and related stress fields*, Geol. Soc. Am. Bull., 106, 1107–1120.
- LAVECCHIA, G., FERRARINI, F., BROZZETTI, F., DE NARDIS, R., BONCIO, P., and CHIARALUCE, L. (2012), *From surface geology to after-shock analysis: Constraints on the geometry of the L'Aquila 2009 seismic fault system*. Ital. J. Geosci. (Boll. Soc. Geol. It.), 131, 330–347, doi:10.3301/IJG.2012.24.
- LAVECCHIA, G., MINELLI, G., and PIALI, G. (1988), *The Umbria-Marche arcuate fold belt (Italy)*, Tectonophysics, 146, 125–137.
- MEGHRAOUI, M., BOSI, V., and CAMELBECK, T. (1999). *Fault fragment control in the 1997 Umbria-Marche, central Italy, earthquake sequence*, Geophys. Res. Lett., 26, 1069–1072.
- MONTONE, P., MARIUCCI, M.T., and PIERDOMINICI, S. (2012). *The Italian present-day stress map*. Geophys. J. Int., 189, 705–716.
- PACE, B., BONCIO, P. and LAVECCHIA, G. (2002), *The 1984 Abruzzo earthquake (Italy): an example of seismogenic process controlled by interaction between differently oriented synkinematic faults*, Tectonophysics, 350, 237–254.
- PIERDOMINICI, S. and HEIDBACH, O. (2012), *Stress field of Italy-Mean stress orientation at different depths and wave-length of the stress pattern*. Tectonophysics, 532–535, 301–311.
- PINO, N.A., and DI LUCCIO, F. (2009), *Source complexity of the 6 April 2009 L'Aquila (central Italy)9 earthquake and its strongest aftershock revealed by elementary analysis*, Geophys. Res. Letters, 36, L23305.
- PIZZI, A., and GALADINI, F. (2009), *Pre-existing cross-structures and active fault segmentation in the northern-central Apennines (Italy)*, Tectonophysics, 476, 304–319.
- PONDRILLI, S., MORELLI, A., EKSTRÖM, G., MAZZA, S., BOSCHI, E., and DZIEWONSKI, A.M. (2002), *European-Mediterranean regional*

- centroid-moment tensors: 1997–2000*, Phys. Earth Planet. Inter., 130, 71–101.
- ROMANO, M.A., DE NARDIS, R., GARBIN, M., PERUZZA, L., PRIOLO, E., LAVECCHIA, G., and ROMANELLI, M. (2013). *Temporary seismic monitoring of the Sulmona area (Abruzzo, Italy): a quality study of microearthquake locations*. Nat. Hazards Earth Syst. Sci., 13, 2727–2744, 2013.
- ROVIDA, A., CAMASSI, R., GASPERINI, P., and STUCCHI, M. (a cura di) (2011), CPTI11, la versione 2011 del Catalogo Parametrico dei Terremoti Italiani. Milano, Bologna, <http://emidius.mi.ingv.it/CPTI>. doi:10.6092/INGV.IT-CPTI11.
- SPERNER, B., MÜLLER, B., HEIDBACH, O., DELVAUX, D., REINECKER, J., and FUCHS, K. (2003), Tectonic stress in the Earth's crust: advances in the World Stress Map project. In: NIEUWLAND, D.A. (ed.) NEW INSIGHTS INTO STRUCTURAL INTERPRETATION AND MODELLING, J. Geol. Soc. London, Special Publications, 212, 101–116.
- TWISS, R.J., and UNRUH, J.R. (1998), *Analysis of fault slip inversions: Do they constrain stress or strain rate?*, J. Geophys. Res., 103, 12205–12222.
- VALENSISE, G., and PANTOSTI, D. (2001), *The investigation of potential earthquake sources in peninsular Italy: A review*, J. Seismol., 5, 287–306.
- VALOROSO, L., CHIARALUCE, L., PICCININI, D., DI STEFANO, R., SCHAFF, D., WALDHAUSER, F. (2013), *Radiography of a normal fault system by 64,000 high-precision earthquake locations: The 2009 L'Aquila (central Italy) case study*, J. Geophys. Res., B: Solid Earth, 118, 1156–1176.
- VITTORI, E., DEIANA, G., ESPOSITO, E., FERRELLI, L., MARCHEGIANI, L., MASTROLORENZO, G., MICHETTI, A.M., PORFIDO, S., SERVA, L., SIMONELLI, A.L., and TONDI, E. (2000), *Ground effects and surface faulting in the September-October 1997 Umbria-Marche (central Italy) seismic sequence*, J. Geodyn., 29, 535–564.

(Received September 6, 2013, revised September 1, 2014, accepted September 2, 2014)